RATIONAL DESIGN OF PROTEIN KINASE A PHOSPHORYLATION SWITCHES

by
Allen Kyung Kim

A dissertation submitted to Johns Hopkins University in conformity with the requirements for the degree of Doctor of Philosophy

Baltimore, Maryland
September 2019

Abstract

Phosphorylation is an important post-translational modification, known for its dynamic role in cellular signal transduction networks. Its most salient feature is its ability to change important properties of proteins such as protein-protein interaction and localization. This dissertation focuses on two types of localization sequences rich in basic residues that can be regulated by phosphorylation: 1) plasma-membrane-targeting sequence and 2) nuclear localization sequence. Phosphorylation in this region leads to a disruption of the electrostatic interaction necessary to target the protein to the correct localization. By using the substrate recognition mechanism of basophilic kinases, this dissertation demonstrates it is possible to embed phosphate acceptors into localization sequences to create a kinase switch. In the case of the plasma-membrane-targeting sequence, this principle was used to explore parameters of the switching mechanism found in the C-terminus of K-Ras4b that was previously not possible due to constraints of Protein Kinase C substrate phosphorylation. In the second part of this work, the principles were used to design a nuclear-cytosol translocation reporter for Protein Kinase A, which performs comparably in dynamic range and kinetics to existing FRET reporter. This work collectively demonstrates that phosphorylation switching mechanisms reported in literature can be reconstituted from first principles.

Thesis Committee: Takanari Inoue (Advisor), Taekjip Ha, Sergi Regot

Acknowledgments

I would like to thank Takanari Inoue for providing the resources and environment to carry out my dissertation work. I would also like to thank my committee members—Taekjip Ha and Sergi Regot, whose inputs and works have largely shaped and motivated this dissertation's direction. Over the last 6 years, I had the pleasure of getting to know all the Inoue Lab members and being part of the lively discussions that comprise the lab meetings. I would like to express appreciation to the current lab members for the camaraderie and insights—Jack Mountain, Hideki Nakamura, Yuta Nihongaki, Kester Coutinho, Helen Wu, Hideaki Matsubayashi, and Abhijit Deb Roy. I also had the pleasure of getting to know all the former lab members who are no longer present—Elmer Rho, Allister Suarez, Siew Cheng Phua, Yu-Chun Lin, Steven Su, Shiva Razavi, Yuchuan Miao, Jackie Niu, and Takafumi Miyamoto. It was also a great joy to work together with the undergraduate and high school students that have come through the lab—Gayatri Pillai, Zi-Yi Choo, and Yoav Kargon. They were all immensely talented and were all much more proficient in laboratory work than I was when I first started. Last but not least, I would like to make a special mention of Robert Derose, the lab manager, who does the thankless, day in and day out.

I also want to express my appreciation for Ivan Bazarov, Professor of Physics at Cornell University. As an undergraduate, I had never considered scientific research as a serious career path until I worked with him. He placed a disproportionate and undeserved amount of trust in me and my abilities. I am grateful to him for all these things and helping me open my eyes to science. I would not have made the decision to pursue a PhD without him.

Lastly, I would like to thank my parents. I do not have any doubts that I won the parent lottery. I believe that it takes a tremendous amount of patience, wisdom, and courage to view your children as individuals and not as extensions of oneself. My parents have been relentlessly

supportive of my decisions, even when they did not agree with me. There are no words to describe the level of gratitude I feel for knowing that they are always there for me.

Table of Contents

Abstract ii

Acknowledgments iii

List of Figures vii

1. Introduction 1

2. Rational Design of a Protein Kinase A Farnesyl-electrostatic Switch 6

Introduction 6

Materials and Methods 7

Cell Culture and Transfection 7

Image Acquisition 7

Image Analysis 8

Colocalization Analysis 8

Statistical Analysis 9

DNA Cloning 9

Results 10

Discussion 13

3. Rational Design of a Protein Kinase A Nuclear-cytosol Translocation Reporter 22

Introduction 22

Materials and Methods 23

Cell Culture and Transfection 23

Image Acquisition 24

Image Analysis 24

DNA Cloning 25

Results 26

Discussion 28

4. Conclusion 40

5. References 42

6. Curriculum Vitae 49

List of Figures

Figure 2-1: Basic design of the synthetic farnesyl-electrostatic switch. 15

Figure 2-2: Effects of substrate valency and positive charge content on FES-PKA localization and response 17

Figure 2-3: Role of positively charged residues in phosphorylation-dependent translocation. 19

Figure 2-4: Response of FES-PKA to Ca^{2+} influx and comparison of FES-PKA to AKAR3EV. 21

Figure 3-1: Basic design of the PKA kinase reporter. 30

Figure 3-2: Effects of valency on initial localization and response to PKA activation. 31

Figure 3-3: Effects of addition of NES on initial localization and response to PKA activation. . 33

Figure 3-4: Duplex monitoring of PIP_3 and PKA in a single cell. 35

Figure 3-5: Response of tetravalent substrate to PKA activation. 37

Figure 3-6: Duplex monitoring of PIP_3 and PKA in a single cell with PKA activation followed by EGF treatment. 38

1. Introduction

The central dogma, which states that information that is stored in DNA is translated to proteins through RNA, is one of the foundational bases for how we understand living cells[1]. At the core of the central dogma is the assumption that a cell's ability to survive and proliferate is encoded in a molecular form in DNA and is passed down from generation to generation. However, this genetic information is generally considered a static entity and does not sufficiently explain how cells are able to maintain survival on a shorter timescale.

The cell's ability to actively respond to external stimuli and adapt is an important part of a cell's survivability. This is generally understood to be found at the level of the proteins, where the diverse types of proteins and their dynamic interactions can control almost every aspect of a cell. Proteins themselves are not static entities, and post-translational modifications, which are chemical groups covalently modified onto proteins, can control important properties of proteins including their interactions with other molecules and their conformation[2]. At the proteome-level, these post-translational modifications can be viewed to be the workhorse of a cell's signal transduction network.

There exist over 200 known post-translational modifications[3]. They can take on the form of small molecules, lipid groups, sugar molecules, or other proteins. For instance, the addition of small lipid groups such as palmitoyl or myristoyl are often involved in trafficking and anchoring of proteins to the lipid bilayer in the cell[4], while acetylation or ubiquitination can control protein stability amongst other roles inside a cell[5,6]. Of these post-translational modifications, the most well-known post-translational modification is phosphorylation.

Phosphorylation is the addition of a phosphate group to serine, threonine, or tyrosine in eukaryotes by a kinase. As with all reversible post-translational modifications, the phosphorylation status of a given protein is determined by the net balance of kinase and phosphatase activity. In the case of phosphorylation, it is generally understood that it is the activation of the kinase that drives phosphorylation, not the deactivation of phosphatases.

This important property is supported by the observation that there are 200 known human phosphatases to 500 known kinases[7,8]. Furthermore, the substrate recognition pattern (or the consensus sequence) is much more well-characterized for kinases than phosphatases. These identifications of kinases have arisen from genomic studies and are based on sequence alignments of the catalytic subunit, which characteristically defines a kinase. Furthermore, kinases can be broadly classified based on various properties, one of which is the mechanism of substrate recognition.

Substrate recognition is an important property of phosphorylation that prevents all potential phosphate acceptors from being indiscriminately phosphorylated[9]. There are three known modes of substrate recognition defined by the types of amino acids surrounding a phosphate acceptor: 1) basophilic, 2) acidophilic, and 3) proline-directed. Biophysically, molecular interactions between the catalytic subunit of the kinase and the substrate is generally considered important for ensuring binding between the substrate and the catalytic subunit of the kinase. For this reason, the amino acids surrounding the phosphate acceptor can be used as a strong predictor of which kinases will phosphorylate which substrate sequences. Numerous studies have used this very principle to determine consensus sequences for various kinases by building peptide libraries which are then phosphorylated with a kinase of interest[10–12]. The phosphorylated peptides can then be enriched and sequenced through Edman degradation. This *in vitro* method of determining consensus

sequences have been powerful in characterizing the consensus sequence many of the AGC kinases (such as Akt, Protein Kinase A, and Protein Kinase C).

More importantly, although consensus sequences may suggest otherwise, the ability for a substrate to be phosphorylated is not a binary parameter. Changes in key amino acids in the substrate sequence can substantially change a substrate's ability to become phosphorylated. For this reason, the phosphorylation kinetics of any given substrate is traditionally defined by the Michaelis-Menten parameters, V_m (maximum velocity of a reaction) and K_m (concentration at half-max velocity). In the case of Protein Kinase A, it is generally understood that arginines in P-2 and P-3 positions are what defines substrates of this kinase. A study by Kemp, et al. in 1977 showed that changing the amino acid at the P-2 position from arginine to lysine maintains a comparable V_{max} as the ideal substrate (LRRASLG), while only increasing the K_m approximately 16-folds[13]. Although consensus sequences would suggest otherwise, the peptide with the lysine in the P-2 position could be a potential physiological substrate. This is largely because cells have mechanisms by which the effective concentration of a protein can be increased allowing it to surpass the biochemical threshold for phosphorylation, for instance, by membrane anchoring[14] or through phase separation[15].

One of the key takeaways from these studies is that a consensus sequence analysis has a bias towards the amino acids responsible for the strongest of substrate-kinase interactions. In 1996, Karin and co-workers demonstrated an exception to this consensus sequence understanding of phosphorylation. In c-Jun, a substrate of JNK, the amino acid sequence necessary for phosphorylation was discovered to be much further away from the phosphate acceptor[16]. These sequences were referred to as docking sequences, which increased the effective concentration, without directly changing the biochemical property of the interaction that occurs between the

catalytic subunit of the kinase and the amino acids surrounding the phosphate acceptor. This property has been generally observed in many other kinase-substrate pairs, most well known in the mitogen-activated protein kinases[17,18]. An important implication of this finding is that a kinase can phosphorylate a substrate that has a much weaker substrate recognition motif, if there are docking sequence to increase its effective concentration.

Phosphorylation's importance in biology is its ability to change important properties of a protein such as their localization. One of such examples is found in the C-terminus of K-Ras4b, a small GTPase upstream of PI3K and MAPKKK pathway, where two sequencing motifs are responsible for targeting to the protein to the plasma membrane[19]. The first is the -CAAX motif which anchors the protein to the cellular membrane system. This alone is insufficient to target the protein to the plasma membrane. Thus, there is a cluster of positively charged residues near the -CAAX motif which directs the protein to the plasma membrane, presumably through the interactions with negatively charged lipids in the inner leaflet of the plasma membrane. The extent to which a protein is enriched at the plasma membrane, in respect to the intracellular membranes, is determined by the positive charge content in this region. Phosphorylation in this region leads to a redistribution of K-Ras4b. It is known that a GAP-insensitive mutant of K-Ras4b(G12V) induces apoptosis through this switching mechanism[20].

Similarly, nuclear localization sequences rely on the presence of basic residues for their signaling property[21,22]. The canonical localization sequence relies on the presence of a cluster of basic residues. Although there are different classifications based on the exact arrangement of these residues, in general, greater number of positive charges in these clusters leads to a stronger localization in the nucleus. The actual machinery of nuclear localization occurs through facilitated diffusion where the nuclear-localization-sequence-containing protein is bound to importin-α,

which is then released inside the nucleus mediated by the GTP-bound form of the small GTPase, Ran. This targeting effect can be diminished through phosphorylation[23,24].

In both localization sequences, electrostatic interaction through basic residues is the key mode by which the targeting is achieved. For this reason, introducing phosphate groups (through phosphorylation) into these regions can decrease the targeting efficiency by reducing the positive charge content. This dissertation focuses on the development of switches built on the observation that the substrate recognition mechanism of Protein Kinase A can be used to design *de novo* targeting sequences that contain phosphate acceptors 1) in plasma-membrane-targeting sequence in -CAAX proteins and 2) in nuclear localization sequences.

2. Rational Design of a Protein Kinase A Farnesyl-electrostatic Switch

Introduction

Dramatic shift in protein localization can be induced by post-translational modifications at localization sequences. In the case of K-Ras4b, the localization sequence is found in the C-terminus where the combination of polybasic residues and the -CAAX motif (where C is cysteine, A is aliphatic residue, and X is any residue) targets the protein to the plasma membrane. The -CAAX motif serves as a signal for enzymatic processing (involving farnesyltransferase, Ras-converting enzyme I, and isoprenylcysteine carboxyl methyltransferase) that leads to the attachment of a farnesyl group[25–27]. As farnesylation alone is not sufficient for plasma membrane targeting, many plasma-membrane-targeted farnesylated proteins including K-Ras4b also require the presence of a cluster of positively charged residues near the -CAAX motif[28–33].

Studies have shown that Protein Kinase C phosphorylation of serine-181 leads to a disruption of K-Ras4b's localization at the plasma membrane[34,35]. Schmick, et al. has shown that the electrostatic interaction between the positively charged residues in the protein and the negatively charged lipids in the plasma membrane is responsible for biasing the trafficking of K-Ras4b to the plasma membrane[36]. Phosphorylation in this region removes this bias by disrupting the favorable electrostatic interaction (Fig. 2-1A), a mechanism known as the farnesyl-electrostatic switch.

Characterizing the farnesyl-electrostatic switch mechanism has technical limitations, as changing the positively charged residues of the C-terminus of K-Ras4b directly affects its phosphorylability. We have overcome this limitation by designing a farnesyl-electrostatic switch using a known substrate sequence of Protein Kinase A (PKA). Unlike Protein Kinase C which

requires a cluster of positively charged residues for substrate recognition[11], PKA requires only two arginines[37,38]. This allowed us to modulate the positive charge content of the switch in a substantial manner, while preserving phosphorylability, allowing us to explore parameters of the farnesyl-electrostatic switch that was previously not possible.

Materials and Methods

Cell Culture and Transfection

HeLa (CCL-2, ATCC, Manassas, VA) cells were routinely passaged and cultured in DMEM (10-013-CV, Corning, Corning, NY) supplemented with 10% FBS (F2442, Sigma, St. Louis, MO) and maintained at 37°C in 5% CO_2. For imaging experiments, cells were seeded at a 30-40% confluence on a #1 coverslip (48380-080, VWR, Radnor, PA) placed inside 6-wells (353046, Corning, Corning, NY). Cells were transfected next day with FugeneHD (E2311, Promega, Madison, WI) at a ratio of 1:1 according to manufacturer's protocol, and 50 ng of DNA was added dropwise into each well. Cells were serum-starved with DMEM (17-205-CV, Corning, Corning, NY) without phenol red and supplemented with 2 mM L-glutamine (25-005-CL, Corning, Corning, NY) morning of the following day. In the afternoon of the same day, cells were imaged by transferring the coverslip to an Attofluor cell chamber (A7816, Invitrogen, Carlsbad, CA).

Image Acquisition

Images were acquired on an inverted microscope (IX81, Olympus, Tokyo, Japan) with a heated chamber that maintained conditions of 37°C and 5% CO_2 (WELS, Tokai-Hit, Fujinomiya, Japan). Images were acquired for 15 minutes or 25 minutes, as noted, at 1-minute interval. After 5 minutes, cells were treated with either 50 µM forskolin (F6886, Sigma, St. Louis, MO) and 100 µM IBMX (I5879, Sigma, St. Louis, MO) cocktail or 1 µM ionomycin (I-6800, LC Laboratories,

Woburn, MA), as noted. Images were acquired with CMOS camera (C11440, Hamamatsu Photonics, Hamamatsu, Japan) on a 60x oil objective (60x PlanApo N, Olympus, Tokyo, Japan). Microscope was controlled with MetaMorph (Molecular Devices, San Jose, CA) with motorized stage controller (MS-2000, ASI, Eugene, OR) and filter wheel controller (Lambda 10-3, Sutter Instrument, Novato, CA). The sample was illuminated with a LED light source (pE-300, CoolLED, Andover, UK). For FRET experiments, images were acquired by exciting with CFP and detecting in the YFP channel. All experiments shown in a given panel were performed together.

Image Analysis

The signal at the intracellular membranes was quantified by co-expressing in cells an endomembrane marker that consisted of a prenylation sequence with no basic residues. ImageJ (NIH, Bethseda, MD) was used to track a 15x15 pixel (4.66 pixel = 1 μm) square region that contained the greatest average fluorescence intensity of the endomembrane marker. For fluorescence quantification, the background was subtracted, and the response of the signal was calculated by taking the ratio of signal with the average of the pre-treatment signal at the region of interest determined with the endomembrane marker. For FRET quantification, the background was subtracted, and the YFP emission signal was divided by the CFP emission signal. The reported response is this quantity normalized by the average of the pre-treatment signal for the whole cell.

Colocalization Analysis

For colocalization analysis, the role of the two polybasic residues clusters were characterized by mutating the positively charged residues to alanines, respectively. Cells were co-transfected with the mutated peptide and an unmutated peptide, both unphosphorylable. The extent of the colocalization between the two peptides was analyzed by first calculating a 20x20 pixel median filtered image for each channel and respectively subtracting them from the original images.

The two background-subtracted images were correlated using Pearson's correlation. The average of these Pearson's correlation from 30 cells is shown in Fig. 2-3D.

Statistical Analysis

Paired Student's t-test was used to test for statistical significance in Fig. 2-1D. Unequal variance t-test was used to test for statistical significance in Figs. 2-2C, 2-2E, 2-3B, 2-3D, and 2-4B. For each analysis, sample size was 30 cells collected over 3 independent experiments (10 cells each). All error bars represent mean±SEM.

DNA Cloning

DNA constructs were cloned by inserting annealed oligonucleotides into EYFP-C1 (Takara Bio, Kusatsu, Japan) and mCherry-C1 (Takara Bio, Kusatsu, Japan) at the SacII and BamHI site. The forward sequences of the inserted oligonucleotides with the restriction sites are as follows:

DNA construct	**cDNA sequence**	**Amino acid sequence**
Endomembrane Marker	GGGCcagcagcagcagcagaccaagtgcgtgatcatgTAGG	QQQQQQTKCVIM
FES-PKA (Unmutated)	GGGCctgagaagagccagcctgggcaagagaagagccagcctgggcaccaagtgcgtgatcatgTAGG	LRRASLGKRRASLGTKCVIM
FES-PKA (Monovalent)	GGGCctgagaagagccagcctgggcaccaagtgcgtgatcatgTAGG	LRRASLGTKCVIM
FES-PKA (Trivalent)	GGGCctgagaagagccagcctgggcaagagaagagccagcctgggcaagagaagagccagcctgggcaccaagtgcgtgatcatgTAGG	LRRASLGKRRASLGKRRASLGTKCVIM
FES-PKA (3 lysines)	GGGCctgagaagagccagcctgggcaagaagaagagaagagccagcctgggcaccaagtgcgtgatcatgTAGG	LRRASLGKKKRRASLG TKCVIM
FES-PKA (5 lysines)	GGGCctgagaagagccagcctgggcaagaagaagaagaagagccagcctgggcaccaagtgcgtgatcatgTAGG	LRRASLGKKKKKRRASLG TKCVIM
FES-PKA (A-A mutant)	GGGCctgagaagagccgccctgggcaagagaagagccgccctgggcaccaagtgcgtgatcatgTAGG	LRRAALGKRRAALGTKCVIM
FES-PKA (S-A mutant)	GGGCctgagaagagccagcctgggcaagagaagagccgccctgggcaccaagtgcgtgatcatgTAGG	LRRASLGKRRAALGTKCVIM
FES-PKA (A-S mutant)	GGGCctgagaagagccgccctgggcaagagaagagccagcctgggcaccaagtgcgtgatcatgTAGG	LRRAALGKRRASLGTKCVIM

FES-PKA (PBR #1 mutant)	GGGCctggccgccgccgccctgggcaagagaag agccgccctgggcaccaagtgcgtgatcatgTAGG	LAAAALGKRRAALGT KCVIM
FES-PKA (PBR #2 mutant)	GGGCctgagaagagccgccctgggcgccgccgc cgccgccctgggcaccaagtgcgtgatcatgTAGG	LRRAALGAAAAALGT KCVIM

Results

Current understanding suggests that the farnesyl-electrostatic switch can be distilled into the following three basic components (Fig. 2-1B): 1) series of positively charged-residues that will electrostatically interact with negatively charged lipids in the plasma membrane, 2) phosphorylation sites that will change positive charge content to regulate signaling, and 3) -CAAX motif that will serve as a recognition sequence for farnesylation. In this study, we utilize these principles observed in the C-terminus of K-Ras4b to design a farnesyl-electrostatic switch that responds to PKA activation.

In our design of the PKA farnesyl-electrostatic switch, we mimicked this general pattern that we observed in K-Ras4b. We utilized a short PKA substrate sequence, Kemptide (LRRASLG), to serve as a source of phosphoserine[37]. We flanked a single lysine with the two Kemptide sequences, and a single leucine was removed from the second Kemptide sequence to maintain a consecutive sequence of positively charged residues. We, then fused a farnesylation substrate recognition sequence (TKCVIM), previously demonstrated to be sufficient for farnesyltransferase processing [39,40]. This resulted in a peptide design (FES-PKA) that encompassed all the basic properties observed in the C-terminus of K-Ras4b necessary for the switching functionality (Fig. 2-1B).

We expressed FES-PKA fused to EYFP in HeLa cells and noticed an enrichment in the plasma membrane. Upon activation of PKA with a cocktail of 50 μM forskolin (FSK) and 100 μM 3-isobutyl-1-methylxanthine (IBMX), the fluorescent signal redistributed to favor the intracellular

membranes (Figs. 2-1C, 2-1D). The effect was reversible with the treatment of a 40 μM H89, a PKA inhibitor. Quantification was performed as described in the Methods. Line-scans of the micrographs shows the appearance and disappearance of a plasma membrane fluorescent signal (Fig. 2-1E), demonstrating the electrostatic switch mechanism of FES-PKA.

We explored the parameter space of this design to determine how different variables would affect the FES-PKA's response and localization. We initially hypothesized that introducing more phosphorylation sites to the peptide can increase the dynamic range of the FES-PKA's response from PKA stimulation (Fig. 2-2A). To test this hypothesis, we generated a peptide with a single phosphorylation site (monovalent) and a peptide with three phosphorylation sites (trivalent). When co-transfected in cells, the monovalent peptide was largely localized in the intracellular membranes, due to an insufficient positive charge content. The trivalent peptide was observed in the nucleus in soluble form, as it appeared that the Ran machinery was being outcompeted by the farnesyltransferase. Quantification showed minor response from the monovalent peptide after PKA activation (Figs. 2-2B, 2-2C). The trivalent peptide was not included in the quantification due to the observed defects in localization.

We hypothesized that increasing the number of lysines flanked by the two phosphoserines will lead to a diminished response from PKA activation due to the unfavorable positive-to-negative charge ratio. We generated two additional peptides that contained three-lysine and five-lysine linkers, respectively. An increase in the number of lysines led to a concomitant decrease in the response from PKA activation (Figs. 2-2D, 2-2E). We also confirmed that the FES-PKA translocation was due to phosphorylation and not due to perturbation of PKA activity by generating mutants which disrupted phosphorylation (Figs. 2-3A, 2-3B). Mutations of both serines to alanines

yielded no response, while having both serines intact led to the most robust response. Having only one of the serines led to an intermediate response.

In our design, we identified two clusters of basic residues, labeled as PBR #1 and PBR #2 (Fig. 2-3C). Based on the observation that the two serines are flanking PBR #2, we hypothesized that PBR #2 would have a more prominent role as a plasma membrane targeting sequence than PBR #1. We tested this hypothesis by mutating all the positively charged in PBR #1 and PBR #2 to alanines, respectively. As the arginines in P-2 and P-3 position are necessary for substrate recognition by PKA[38,41], mutations of these residues to alanines disrupts the phosphorylability of the substrate. For this reason, the serines were mutated to alanines in this experiment. Cells were co-transfected with the mutated FES-PKA and a non-phosphorylable, non-mutated FES-PKA. Mutations in PBR #1 did not appear to disrupt the initial localization, while mutations in PBR #2 caused a substantial enrichment in the intracellular membranes (Fig. 2-3C). Pearson's correlation was calculated by comparing the unmutated peptide against the three variant peptides (Fig. 2-3D).

Finally, polybasic targeting sequences in farnesylated proteins can be disrupted with calcium influx[33,42–45]. This is thought to occur the through binding of calmodulin, independent of phosphorylation. We performed a similar experiment as previous by treating the cells with 1 μM ionomycin under a condition where the extracellular medium contained 1.8 mM Ca^{2+} (Figs. 2-4A). The time-profile shows the translocation of FES-PKA that is unphosphorylable. Both mutants regardless of the presence of serines responded to the influx of Ca^{2+} (Fig. 2-4B). We also compared the response of FES-PKA to the signal change with AKAR3EV[46], a Förster resonance energy transfer (FRET) sensor for PKA activity, 10 minutes after stimulation (Figs. 2-4C, 2-4D).

Discussion

Our design confirmed some of the previously established observations of the C-terminus of K-Ras4b. The six lysines in the positions 175 to 180 is responsible for serving as the signaling sequence to target the protein to the plasma membrane. Previous studies had already established serine-181 as a phosphate acceptor for Protein Kinase C. Our study further suggested that having two phosphorylation sites leads to a substantially more robust response than a single phosphorylation site (Figs. 2-3A, 2-3B). Based on this line of argument, strong phosphorylation at serine-171 in K-Ras4b by an unknown kinase can lead to a more robust translocation. Under this hypothesis, serine-171 and serine-181 can effectively behave as a logical AND gate that would yield the most robust response when both sites are phosphorylated.

Both K-Ras4b and FES-PKA's interaction with the plasma membrane is mediated by the presence of negatively charged lipids, the depletion of which causes the protein's dissociation from the plasma membrane[30,33,47]. This demonstrates that the farnesyl-electrostatic switch is not driven solely by protein phosphorylation[30,3330,3330,33]. This is further complicated by the observation that PDEδ[48–50] and calmodulin[42–44,51] are known binding partners of K-Ras4b that facilitate trafficking. It is currently unknown what role these proteins may have in the mechanism of the farnesyl-electrostatic switch. Due to FES-PKA's substantial difference in sequence to the C-terminus of K-Ras4b, the peptide described here can be used as a reference to determine the extent of these proteins' roles in the switching mechanism, if any.

To summarize, we have rationally designed a farnesyl-electrostatic switch that responds to PKA activity inside cells. This design is based on basic principles observed in the C-terminus of K-Ras4b where the modulation of positive charges by phosphorylation is the underlying mechanism for translocation. Because of its concise sequence, we envision that it can have further

utility in future studies as a kinase sensor or as a module for perturbing signal transduction pathways.

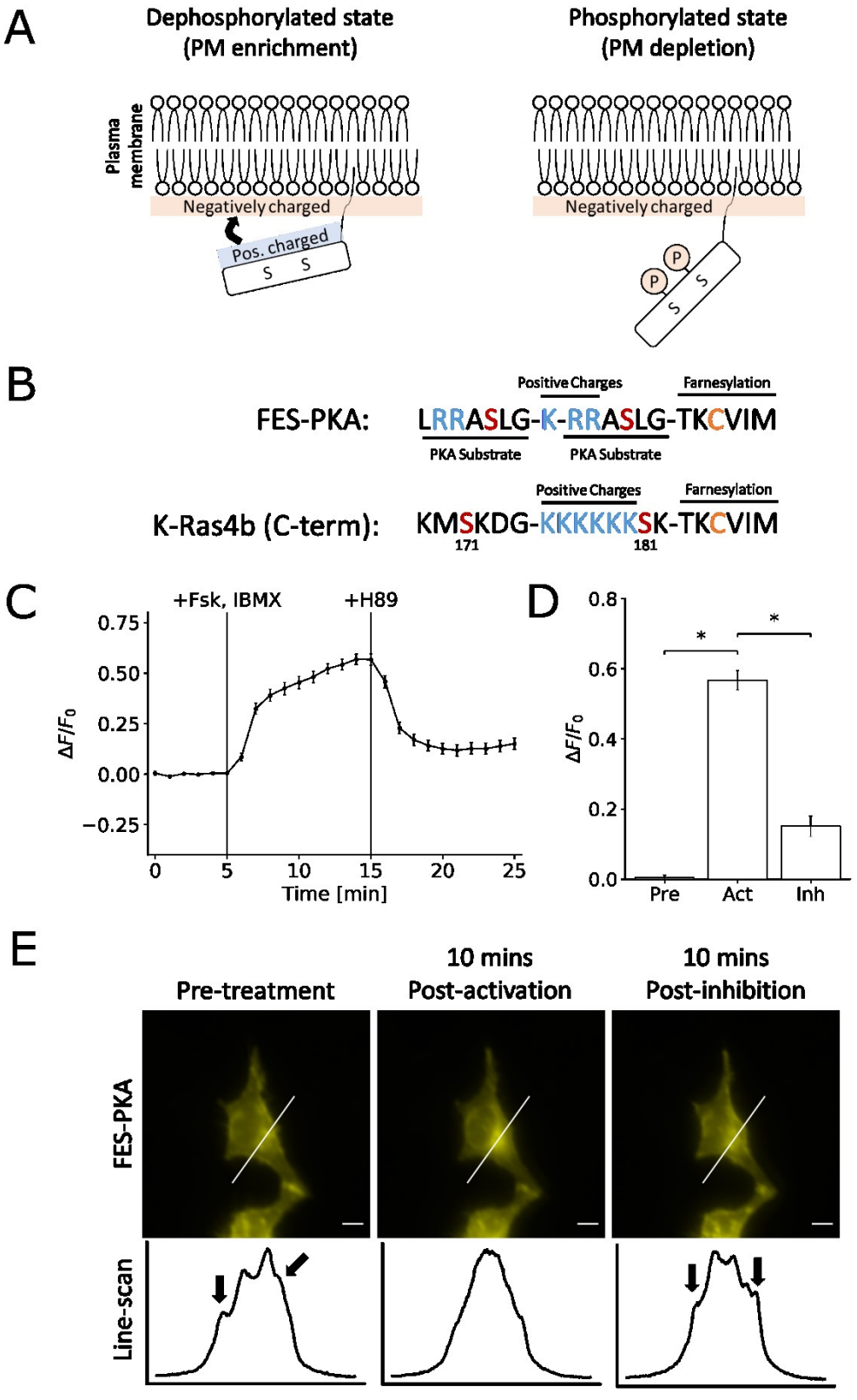
A
Dephosphorylated state
(PM enrichment)
Phosphorylated state
(PM depletion)
Plasma membrane
Negatively charged
Pos. charged
S S
Negatively charged
P
P
S
S
B
Positive Charges
Farnesylation
FES-PKA:
LRRASLG-K-RRASLG-TKCVIM
PKA Substrate
PKA Substrate
Positive Charges
Farnesylation
K-Ras4b (C-term):
KMSKDG-KKKKKKSK-TKCVIM
171
181
C
+Fsk, IBMX
+H89
0.75
0.50
0.25
0.00
−0.25
ΔF/F0
0
5
10
15
20
25
Time [min]
D
0.8
0.6
0.4
0.2
0.0
ΔF/F0
*
*
Pre
Act
Inh
E
Pre-treatment
10 mins
Post-activation
10 mins
Post-inhibition
FES-PKA
Line-scan

Figure 2-1: Basic design of the synthetic farnesyl-electrostatic switch.
(A) Plasma membrane targeting of farnesylated proteins relies on the presence of positively charged residues near the C-terminus. The farnesyl-electrostatic switch relies on the regulation of this sequence through phosphorylation.
(B) C-terminus of K-Ras4b contains a cluster positive charges, two potential phosphate acceptors, and a farnesylation sequence, which was mimicked in the design for the FES-PKA.
(C) Time-profile shows the quantification of the fluorescent signal in response to PKA activation and reversal with PKA inhibition.
(D) Bar chart represents the signal change pre-treatment (at 5 minute), post-treatment with FSK+IBMX (at 15 minutes), and washout with H89 (at 25 min), respectively.
(E) Representative micrographs are shown of cells in the following states: pre-treatment, post-activation, and post-inhibition. Plots below the images show line-scans which reflect the signal intensity along the white line in the micrographs.
All data points in this figure represent an average signal intensity collected from 30 cells over 3 independent experiments (10 cells each), and error bars represents standard error of mean. * represents statistical significance: $p < 0.05$. Scale bar represents 10 μm.

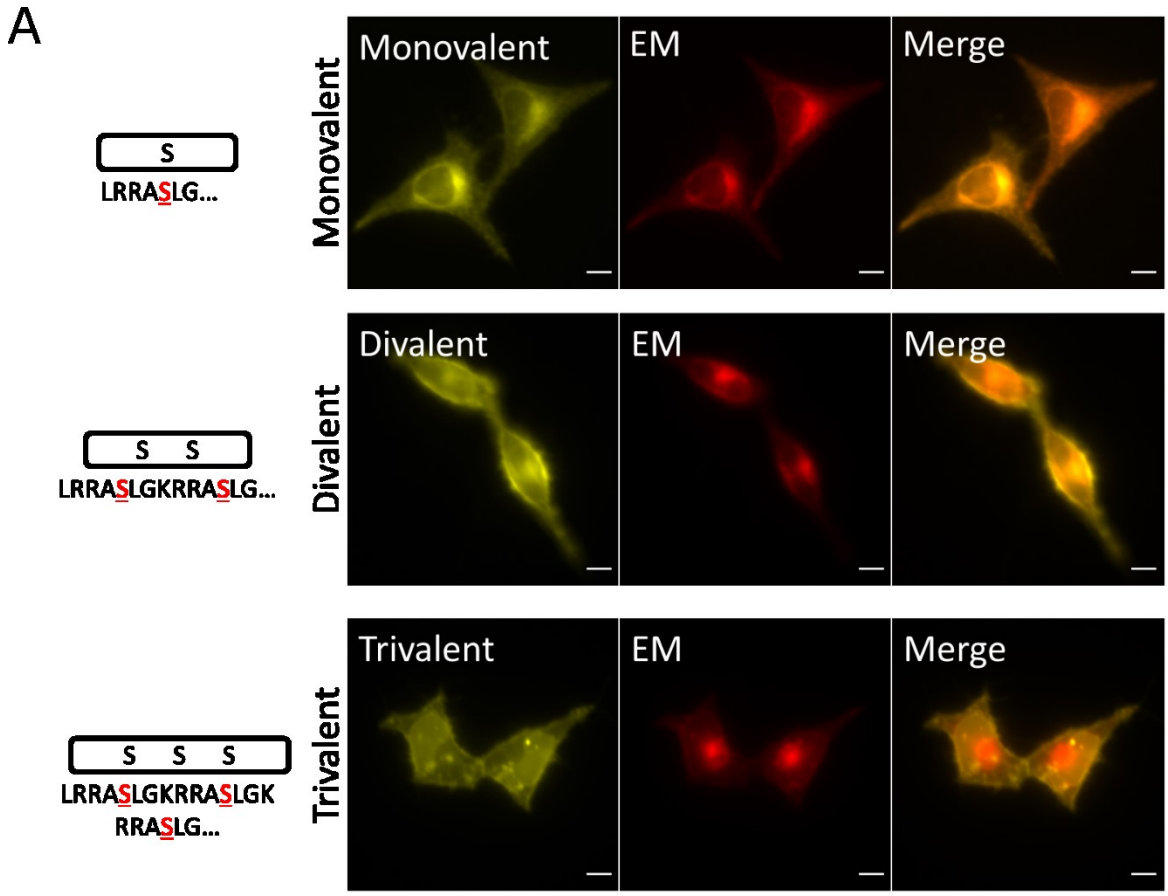
A
S
LRRASLG...
Monovalent
Monovalent
EM
Merge
S S
LRRASLGKRRASLG...
Divalent
Divalent
EM
Merge
S S S
LRRASLGKRRASLGK
RRASLG...
Trivalent
Trivalent
EM
Merge

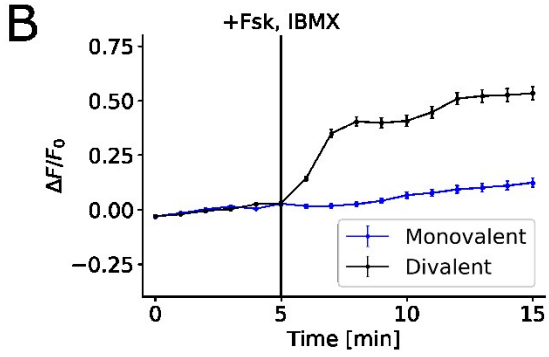
B
+Fsk, IBMX
ΔF/F0
0.75
0.50
0.25
0.00
−0.25
0
5
10
15
Time [min]
Monovalent
Divalent

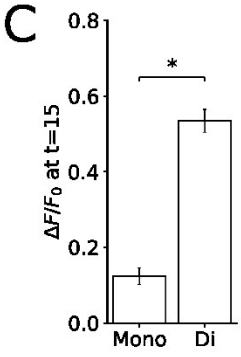
C
ΔF/F0 at t=15
0.8
0.6
0.4
0.2
0.0
*
Mono
Di

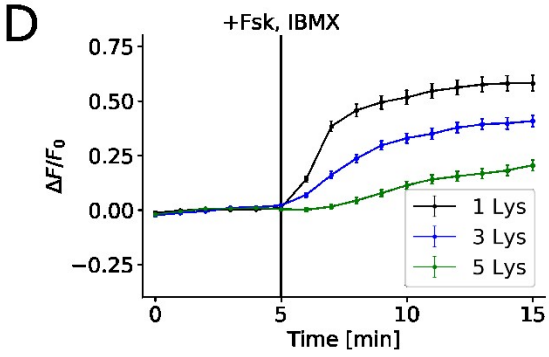
D
+Fsk, IBMX
ΔF/F0
0.75
0.50
0.25
0.00
−0.25
0
5
10
15
Time [min]
1 Lys
3 Lys
5 Lys

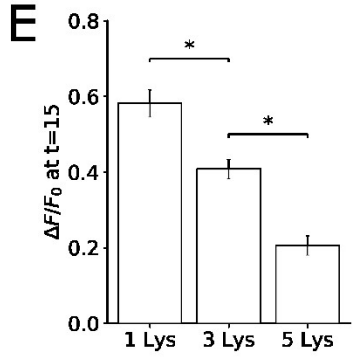
E
ΔF/F0 at t=15
0.8
0.6
0.4
0.2
0.0
*
*
1 Lys
3 Lys
5 Lys

Figure 2-2: Effects of substrate valency and positive charge content on FES-PKA localization and response.

(A) Representative images are shown of cells co-transfected with peptides containing different number of substrates (monovalent, divalent, and trivalent) and an endomembrane (EM) marker. Divalent peptide is shown here as a reference and is the same amino sequence (FES-PKA) as shown in Fig. 1B.

(B) Time-profile shows quantification of fluorescent signal of monovalent and divalent peptides in response to PKA activation. Trivalent peptide was not included in quantification due to localization defects.

(C) Bar chart represents the signal change 10 minutes after PKA stimulation for the monovalent and divalent peptide.

(D) Time-profile shows quantification of fluorescent signal of increasing the positive charge content of the peptide.

(E) Bar chart represents the signal change 10 minutes after PKA stimulation for the three different lysine linkers.

All data points in this figure represent an average signal intensity collected from 30 cells over 3 independent experiments (10 cells each), and error bars represents standard error of mean. * represents statistical significance: $p < 0.05$. Scale bar represents 10 μm.

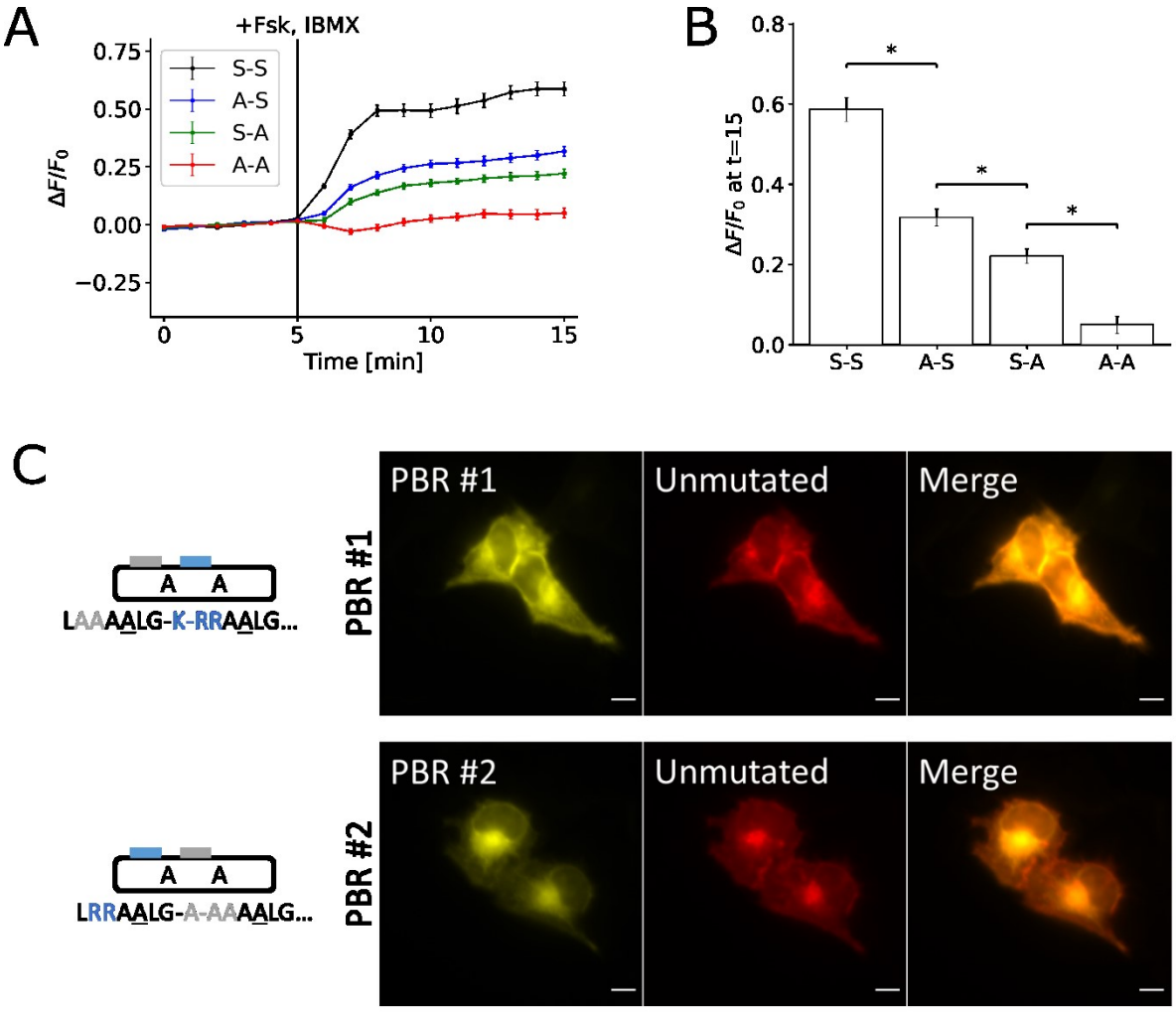
A
+Fsk, IBMX
S-S
A-S
S-A
A-A
ΔF/F0
Time [min]
B
ΔF/F0 at t=15
S-S
A-S
S-A
A-A
C
PBR #1
Unmutated
Merge
A A
LAAAALG-K-RRAALG...
PBR #2
LRRAALG-A-AAAALG...

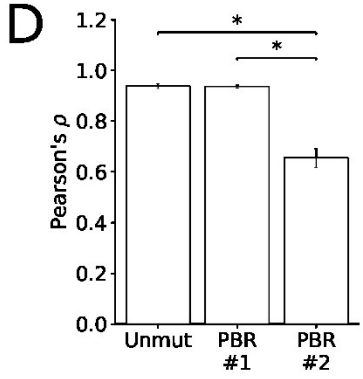
D
Pearson's ρ
Unmut
PBR #1
PBR #2

Figure 2-3: Role of positively charged residues in phosphorylation-dependent translocation.

(A) Time-profile shows quantification of peptides with various permutations of non-phosphorylable FES-PKA. In the notation S-S, the first letter represents whether the first phosphorylation site is mutated, and the second serine represents whether the second phosphorylation site is mutated.

(B) Bar chart represents the signal change for each of the mutations 10 minutes after PKA stimulation. **(C)** Micrograph represents cell images containing mutations disrupting the positively charged residues in the two clusters of basic residues, respectively.

(D) Bar chart represents the average Pearson's correlation calculated by comparing the three different peptides against their unmutated counterpart.

All data points in Figs. 2A and 2B represent data collected from 30 cells over 3 independent experiments (10 cells each), and error bars represents standard error of mean. * represents statistical significance: $p < 0.05$. Scale bar represents 10 μm.

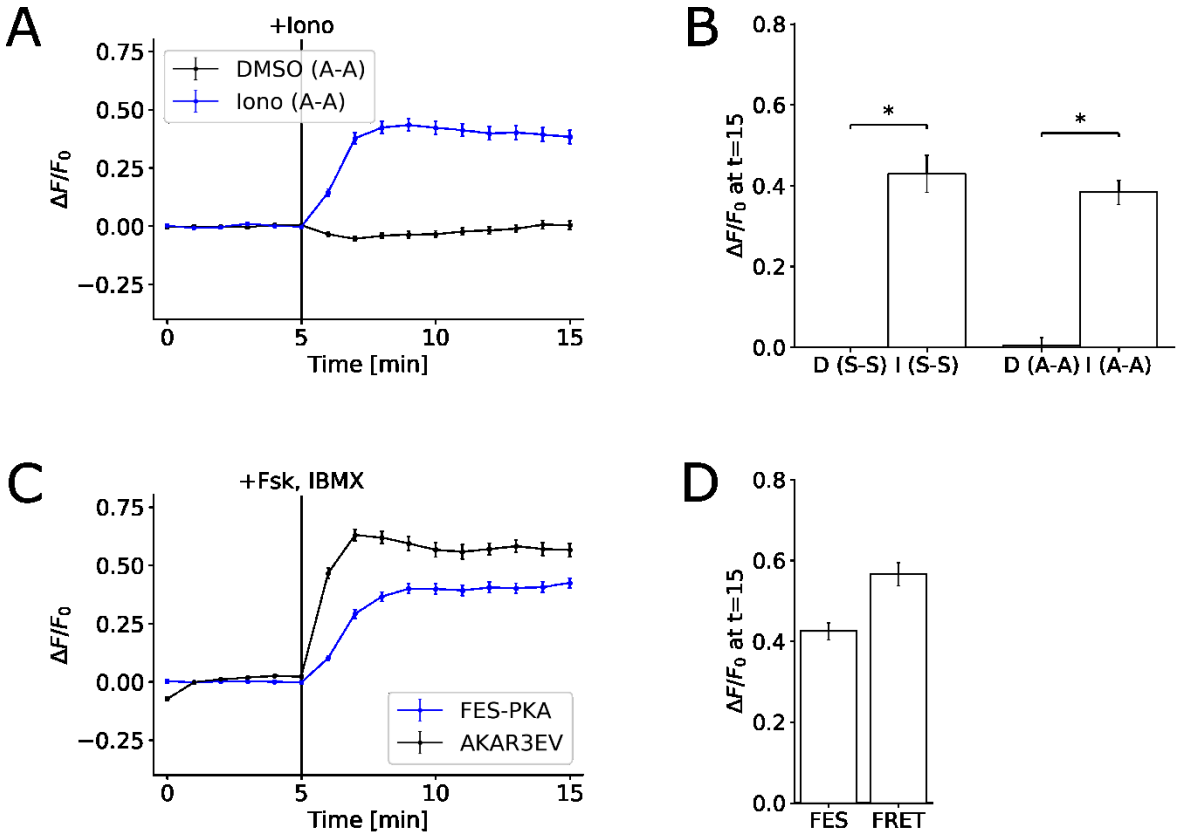

<u>Figure 2-4:</u> Response of FES-PKA to Ca^{2+} influx and comparison of FES-PKA to AKAR3EV.

(A) Time-profile shows quantification of a non-phosphorylable FES-PKA in response to Ca^{2+} influx.

(B) Bar chart represents the signal change of a non-phosphorylable FES-PKA (A-A) and phosphorylable FES-PKA (S-S), respectively, after 10 minutes of treatment with DMSO (D) and ionomycin (I), respectively.

(C) Time-profile shows quantification of FES-PKA response in comparison to a PKA FRET sensor (AKAR3EV) in response to PKA activation.

(D) Bar chart represents the signal change for the FES-PKA (FES) and AKAR3EV (FRET) 10 minutes after PKA activation.

All data points represent an average signal intensity collected from 30 cells over 3 independent experiments (10 cells each), and error bars represents standard error of mean. * represents statistical significance: $p < 0.05$. Scale bar represents 10 µm.

3. Rational Design of a Protein Kinase A Nuclear-cytosol Translocation Reporter

Introduction

As one of the earlier kinases to be characterized, Protein Kinase A (PKA) has been discovered to play an important role in numerous physiological processes including cardiac physiology[52], neuronal development[53], and adipocyte function[54]. The kinase, in its inactive form, exists as a holoenzyme composed of two catalytic subunits and two regulatory subunits. Activation of the kinase is generally understood to occur through the increase of cAMP, which leads to the dissociation of the holoenzyme. Kinase activity can further be spatially regulated through the existence of A-kinase anchoring proteins which anchor the holoenzyme to specific subcellular localizations[55].

This well-characterized nature of PKA has naturally lent to it being used as a platform for number of interesting concepts for kinase reporters. One of the earliest of such designs was the utilization of Förster resonance energy transfer (FRET) to monitor the dissociation of the catalytic and regulatory subunits of the protein, a basic design that was used to demonstrate the localness of cAMP concentration and PKA activity[56]. A more generalizable variant of this design was established by Zhang, et al. which involved creating a chimera that consisted of FRET-compatible fluorescent proteins, a phosphopeptide binding domain, and a short kinase substrate sequence[57]. Upon phosphorylation, the binding affinity between the phosphopeptide binding domain and the substrate sequence dramatically increase leading to a conformational change, which is then measured through changes in FRET. This design has been the basis for number of generations of PKA FRET reporters existing in literature[46,58–61].

One of the main advantages of fluorescent kinase reporters is the ability to analyze kinase activity on a single cell level in real time. Despite this advantage, FRET reporters have the inherent downside of requiring two fluorophores, limiting the ability to monitor multiple kinases simultaneously with most experimental setups. Numerous groups have reported various approaches to overcome this limitation in respect to PKA. These approaches have included using multiple FRET pairs[62], utilizing polarization of light as a readout[63], or designing proteins that changes subcellular localization in response to phosphorylation[64].

In summary, arginines in the P-2 and P-3 positions are important residues for substrate recognition[12,13]. By placing the amino acid sequence for the substrate in tandem with minor modifications, we designed an amino acid sequence that loosely conformed to known consensus nuclear localization sequence (NLS) motifs[21]. This peptide responded to PKA activity by shuttling between the nucleus and the cytosol. We furthermore performed basic optimization and demonstrated its use in simultaneously monitoring two different signals within a cell.

Materials and Methods

Cell Culture and Transfection

HeLa cells were cultured in DMEM with 10% FBS and routinely passaged. Cells were seeded at a density of 2.0×10^4 cells/cm^2 in a 6-well plate containing a 25 mm coverslip one day before transfection. They were transfected with multiple plasmids at an amount of 50 ng each using FugeneHD according to manufacturer's protocol. On the following day, culture media was replaced with serum-free DMEM in the morning. Imaging took place in the afternoon of the same day.

Image Acquisition

Images were acquired on an inverted microscope (IX81, Olympus) with a heated incubator that maintained the chamber at 37° and 5% CO_2 (WELS, Tokai-Hit). Images were acquired for either 15 or 25 minutes at 1-minute interval. Drugs were added at the 5-minute and 15-minute point. PKA activation was achieved through treatment with 50 μM forskolin and 100 μM IBMX, unless otherwise noted. For the experiment demonstrating reversibility, the media was replaced with new media containing 40 μM H89 at the 15-minute point, as residual forskolin and IBMX led to an incomplete inhibition of PKA. Images were acquired with a CMOS camera (C11440, Hamamatsu) in a 60x oil objective (Plan Apo N, Olympus) with the appropriate excitation and emission filters driven by a filter wheel controller. Metamorph was used to control the hardware associated with the microscope which includes the motorized stage (MS-2000, Applied Scientific Instrumentation), filter wheels (Lambda 10-3, Sutter Instruments), and LED light source (pE-300, CoolLED). To measure response with the FRET reporter, cells were excited on the CFP channel, and images were acquired on the YFP channel.

Image Analysis

All cells were co-transfected with H2B-mCherry (Figs 3-1, 3-2, 3-3, 3-5) or H2B-mCerulean3 (Figs 3-4, 3-6) to mark the nucleus. Using the H2B as a mask, ImageJ was used to distinguish cytosolic fluorescent signal from the nuclear signal. The fluorescent signal change was tracked by creating a ratio of cytosol-to-nuclear signal. For FRET experiments, the fluorescent signal was tracked by tracking the ratio from YFP emission to CFP emission. For response profiles, data was normalized by the average of the pre-treatment signals. For all experiments excluding the experiment involving duplex monitoring, analysis was carried out across 3 independent experiments. 10 cells were analyzed from each experiment, resulting in a total of 30 cells analyzed.

Student's t-test for unequal variance was used to test for statistical significance in Figs 3-2D and 3-3D.

DNA Cloning

The cDNA for H2B (gift from Sergi Regot) was amplified by PCR and inserted into NheI and AgeI site of the mCherry-C1 and mCerulean3-C1 vectors (Clontech). YFP-PH(Akt) is a standard PH domain construct for PIP3 labeling. All the reporter variants were inserted into the EYFP-C1 vector (Clontech) at the SacII and BamHI restriction sites using annealed oligonucleotides. The forward sequences of the annealed oligonucleotides are tabulated below:

DNA construct	**cDNA sequence**	**Amino acid sequence**
Substrate	GGGCctgagaagagccagcctgggcTAGG	LRRASLG
$Substrate_2$	GGGCctgagaagagccagcctgggcaagaga agagccagcctgggcTAGG	LRRASLGKRRASLG
$Substrate_3$	GGGCctgagaagagccagcctgggcaagaga agagccagcctgggcaagagaagagccagcctg ggcTAGG	LRRASLGKRRASLGKRRASL G
$Substrate_4$	GGGCctgagaagagccagcctgggcaagaga agagccagcctgggcaagagaagagccagcctg ggcaagagaagagccagcctgggcTAGG	LRRASLGKRRASLGKRRASL GKRRASLG
$Substrate_3$-NesA	GGGCctgagaagagccagcctgggcaagaga agagccagcctgggcaagagaagagccagcctg ggcgtggaccagctgagactggagagactgcag atcgacgagTAGG	LRRASLGKRRASLGKRRASL GVDQLRLERLQIDE
$Substrate_3$(AAA)-NesA	GGGCctgagaagagccgccctgggcaagaga agagccgccctgggcaagagaagagccgccctg ggcgtggaccagctgagactggagagactgcag atcgacgagTAGG	LRRAALGKRRAALGKRRAA LGVDQLRLERLQIDE
$Substrate_3$-NesB	GGGCctgagaagagccagcctgggcaagaga agagccagcctgggcaagagaagagccagcctg ggcgacccccctgcccgtgctggagaacctgaccc tgaagagcTAGG	LRRASLGKRRASLGKRRASL GDPLPVLENLTLKS
$Substrate_3$-NesC	GGGCctgagaagagccagcctgggcaagaga agagccagcctgggcaagagaagagccagcctg ggcaaggtggccgagaagctggaggccctgagc gtgaaggagTAGG	LRRASLGKRRASLGKRRASL GKVAEKLEALSVKE
$Substrate_3$-NesD	GGGCctgagaagagccagcctgggcaagaga agagccagcctgggcaagagaagagccagcctg ggcgccctgcagaagaagctggaggagctggag ctggacgagTAGG	LRRASLGKRRASLGKRRASL GALQKKLEELELDE

Results

We designed a phosphorylation switch based on the basic observation that the PKA substrate can be arranged in tandem to form a NLS. Due to the overlapping nature of the NLS with the phosphate acceptor, phosphorylation of this peptide results in a shift in localization. Our final design consisted of NLS and nuclear export sequence (NES), where the NLS contained the three phosphate acceptors for PKA (Fig 3-1A).

When the reporter was fused to EYFP and transfected in cells, this peptide responded to PKA activation by 50 μM forskolin and 100 μM IBMX by redistributing from the nucleus to the cytosol (Fig 3-1B). When the signal change was quantified by taking the ratio of cytosolic fluorescence signal to nuclear signal, the kinetics and dynamic range was comparable to the FRET reporter, AKAR3EV[46]. The response to 40 μM H89, which resulted in the inhibition of PKA, also revealed a similar kinetics and response to its FRET counterpart. A serine-to-alanine mutation of all the phosphate acceptors led to no response, while removing the NES led to a much slower response to the activation. Representative images show the change in localization of the EFYP within the 3 minutes following PKA activation (Fig 3-1C).

To reach the final design, we first designed a switchable NLS. We utilized the Kemptide (LRRASLG)[13], a well-established PKA substrate, as the working unit of the design, which contains the two arginines in the P-2 and P-3 position considered important for substrate recognition. A monovalent substrate alone does not conform to known NLS. However, placing these sequences in tandem leads to a sequence that conforms loosely to NLS motif (Fig 3-2A). We transfected cells with EYFP fused to various number of substrates. Increasing the number of substrates led to a concomitant increase in nuclear localization (Fig 3-2B). When cells were treated with forskolin

and IBMX, the fluorescent signal redistributed to become more diffuse at the end of 10 minutes of treatment determined by a normalized response profile (Fig 3-2C). The pre-treatment localization and the post-treatment localizations was determined by measuring the ratio of cytosol-to-nuclear fluorescent signal (Fig 3-2D). We also tested a construct containing four substrates. However, because of the strong nuclear localization, there was very little measurable cytosolic signal. For this peptide, we measured the depletion of nuclear signal and observed little difference compared to the construct containing three substrates (Fig 3-5). Given these considerations, the trivalent form was considered optimal. However, the response kinetics of the peptide was substantially slower than its counterpart FRET reporter (Fig 3-1B, blue).

To mitigate this difference in response kinetics, we fused a NES to the trivalent substrate. A previous study established the relative strengths of the various NES's[65]. Using this as a reference, we fused a 13-amino-acid, leucine-rich fragment from FMR1, TFIIIA, RanBP1, and Map2K1 (Fig 3-3A). We observed that three of the four NES's overpowered the NLS (Fig 3-3B). This also translated to a decrease in both response amplitude and kinetics (Figs 3-3C, 3-3D). Amongst the four sequences tested, the NES fragment from FMR1 protein led to a substantial improvement in kinetics and dynamic range in comparison to the peptide lacking a NES. The kinetics and response of this design was comparable to that observed with the FRET reporter (Fig 3-1B, blue).

Lastly, by co-transfecting the PH domain from Akt (mCherry) and the PKA phosphorylation switch (EYFP), we simultaneously monitored the synthesis of PIP_3, a lipid secondary messenger, and the activity of PKA. Upon stimulation with 50 ng/mL EGF, we observed a transient increase in PIP_3, indicated by the translocation of the PH domain from the cytosol to the plasma membrane (Fig 3-4A). This was indicated by the accumulation of PH domain at the

plasma membrane upon activation with EGF but not upon PKA activation (Fig 3-4B). PKA activity as measured by the reporter led to a sustained level of increase upon activation of EGF and saturated with treatment of the forskolin and IBMX cocktail (Fig 3-4C). We also reversed the order of treatment and observed PIP_3 enrichment only when the cells were treated with EGF (Fig 3-6).

Discussion

Our PKA phosphorylation switch is *de novo* amino acid sequence based on simple observations of PKA consensus sequence and NLS motif. Using this information, we designed a switch that reproduced the kinetics measured with a well-established FRET reporter. In contrast to FRET reporters, this type of single-fluorophore reporter frees up a fluorescent color, allowing for an additional channel of analysis. We then demonstrated this capability monitoring two different signaling molecules by overexpressing cells with the PH domain from Akt and the PKA reporter.

A switchable NLS alone did not reproduce the kinetics of PKA activation observed with a FRET reporter. The distribution of a protein observed in a cell is determined by the net flux of the nuclear import and nuclear export transport processes. With peptides containing only NLS's, the nuclear import is driven by facilitated diffusion while nuclear export is driven by passive diffusion. As passive diffusion is slower than facilitated diffusion, the time required to reach steady state is longer, reflected by the decrease in response kinetics. The addition of a NES mitigated this issue. An ideal reporter, thus, should be rate-limited by the kinetics of the underlying phosphorylation not by auxiliary processes.

Another important property of reporters is kinase specificity. In our study, we have used a well-characterized substrate sequence of PKA that has been used in previous FRET reporters[46,58–

[61]. Phosphorylation prediction algorithm, NetPhos3.1[66], strongly suggests PKA as the target kinase for this reporter. Furthermore, based on current literature of AGC kinases, PKA is the only AGC kinase that requires two arginines at P-2 and P-3 position[10–13]. These reports do not rigorously rule out non-specific phosphorylation, as substrates are not necessarily required to conform to consensus sequences. However, given current literature and our data, PKA activity appears to be the driving force behind the shuttling.

We used the interaction of positively charged residues in the substrate sequence to the catalytic subunit of PKA to design the reporter. However, this is not necessarily the only method of achieving specificity. Regot, et al. developed a similar reporter which shuttles between the cytosol and the nucleus using a different strategy[64]. The phosphate acceptors in this reporter are placed in a much weaker, proline-rich substrate recognition sequence derived from c-Jun. The affinity towards the substrate is increased through docking sequences, which elevates the effective concentration of the substrate to the kinase[9,16]. We were unable to observe a measurable response with this PKA reporter. However, we speculate that this reporter design relies on a much weaker interaction with the kinase than our design, requiring a more careful optimization of experimental conditions.

In summary, we have designed a reporter based on a rearrangement of a PKA substrate to create a NLS. In principle, this is generalizable to all basophilic kinases, as this mechanistically relies on disruption of electrostatic interactions through phosphorylation. Due to the single-fluorophore nature of this reporter and its comparable performance to a FRET reporter, we envision that this could find broad applications in studies involving single cell analysis of PKA activity.

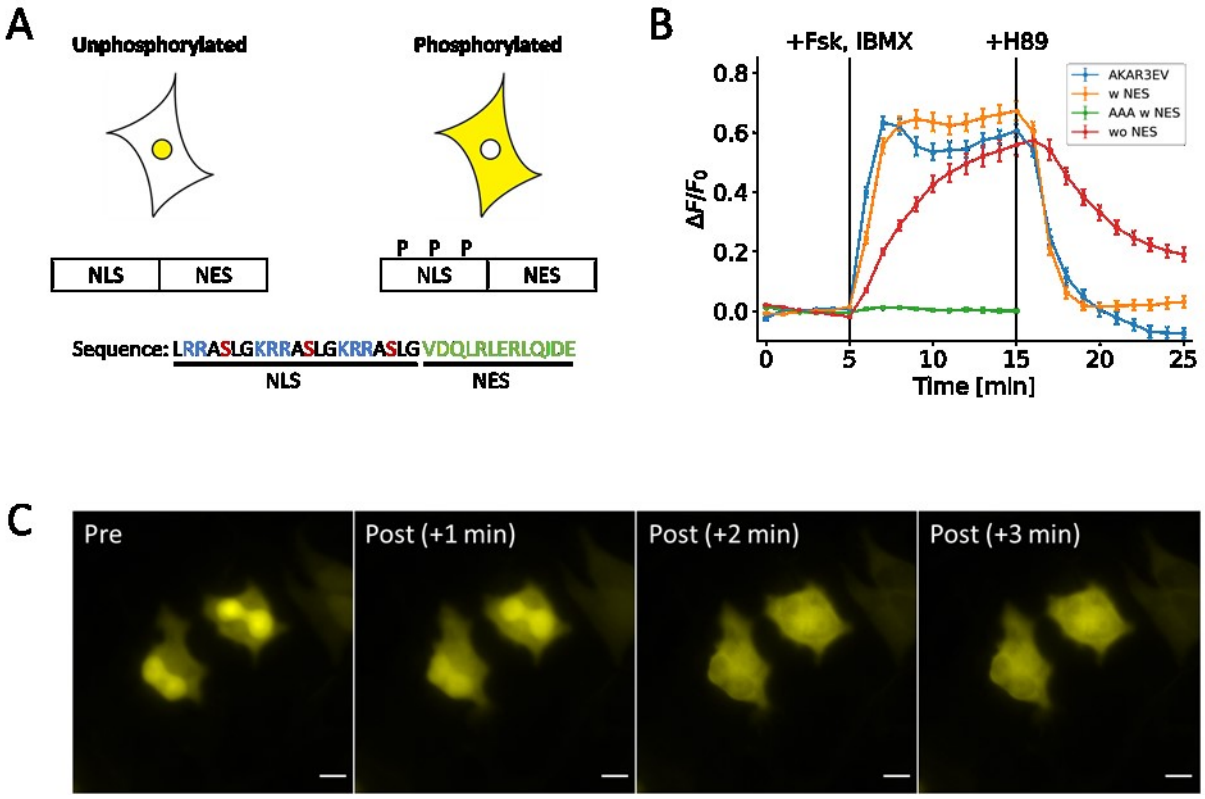

Figure 3-1: Basic design of the PKA kinase reporter.

(A) Design consists of a NLS with three phosphorylation sites fused to a NES sequence. Phosphorylation regulates the activity of the NLS. Basic residues are colored blue; phosphoserine is colored red; and NES is colored green.

(B) Response profile shows the normalized signal change resulting from the activation and inhibition of PKA FRET reporter (blue) and three variants of the nuclear-cytosol translocation reporter. The three variants are: a full version with the NES (yellow), a version lacking the NES (green), and a full version with serine-to-alanine mutations (red).

(C) Representative images show the changes in distribution of the full version of the reporter that occurs within three minutes of PKA activation.

All data points in this figure represent an average signal intensity calculated from 30 cells over 3 independent experiments. Error bar represents standard error of mean. Scale bar represents 10 µm.

A

	Sequence
Sub_1	LRRASLG
Sub_2	LRRASLG-K-RRASLG
Sub_3	LRRASLG-K-RRASLG-K-RRASLG
Sub_4	LRRASLG-K-RRASLG-K-RRASLG-K-RRASLG

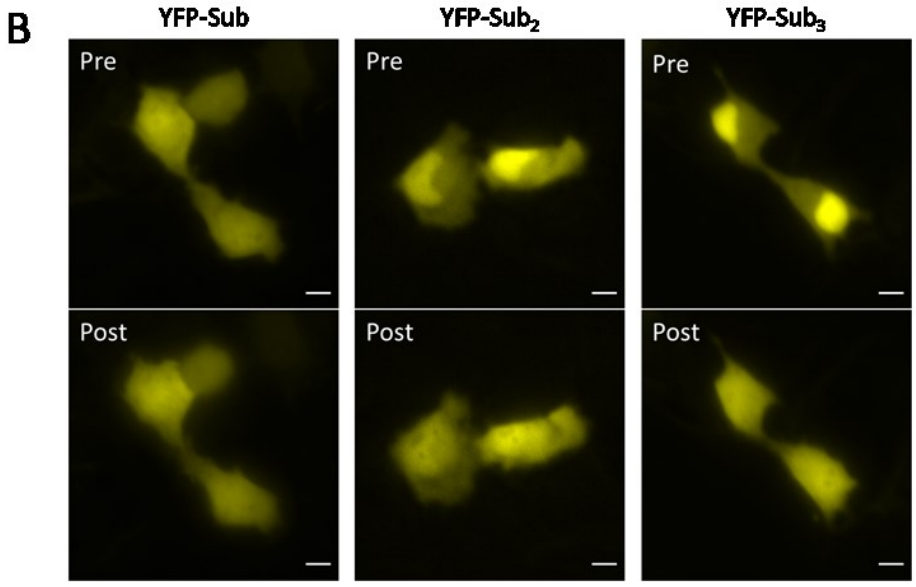

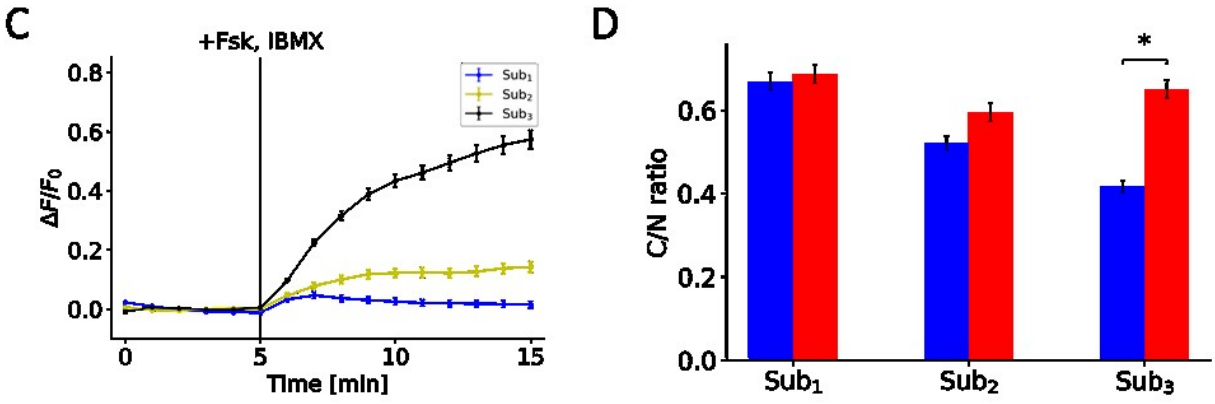

Figure 3-2: Effects of valency on initial localization and response to PKA activation.

(A) Representative images show the initial distribution (Pre) and the distribution 10 minutes post-treatment (Post) for peptides containing one, two, and three substrates.

(B) Response profile shows the normalized signal change resulting from the activation of PKA for peptide consisting of one (blue), two (yellow), and three (black) substrates.

(C) Bar chart represents the pre-treatment localization (blue) and post-treatment localization (red) as measured by taking the ratio of cytosol-to-nuclear fluorescent signal for peptide consisting of one, two, and three substrates.

(D) Table contains the amino acid sequences of the peptides containing the different number of substrates.

All data points in this figure represent an average signal intensity calculated from 30 cells over 3 independent experiments. Error bar represents standard error of mean. * represents $p<0.001$. Scale bar represents 10 μm.

A

	Derived protein	Sequence
NesA	FMR1 (427-439)	VDQLRLERLQIDE
NesB	TFIIIA (328-339)	DPLPVLENLTLK*S
NesC	RANBP1 (179-191)	KVAEKLEALSVKE
NesD	MAP2K1 (32-44)	ALQKKLEELELDE

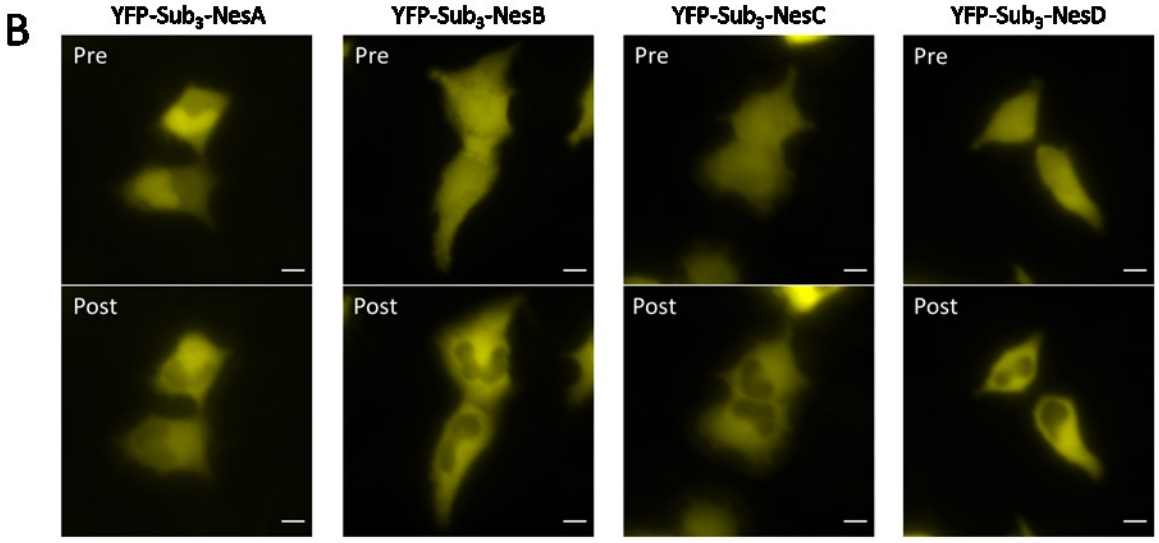

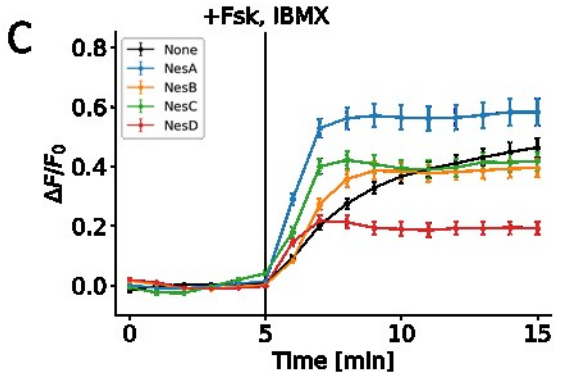

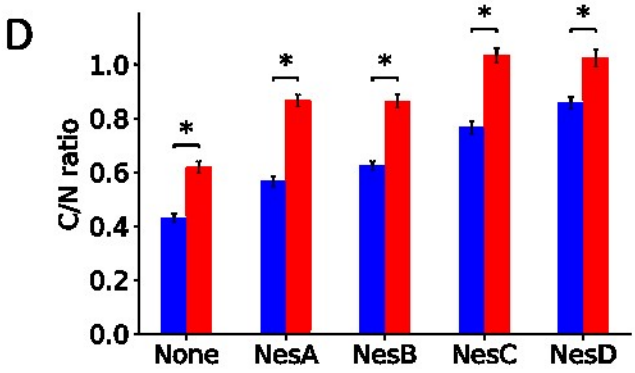

<u>Figure 3-3:</u> Effects of addition of NES on initial localization and response to PKA activation.

(A) Representative images show the initial distribution (Pre) and the distribution 10 minutes post-treatment (Post) for peptides fused with NesA, NesB, NesC, and NesD.

(B) Response profile shows the normalized signal change resulting from the activation of PKA for peptide consisting fused with NesA (blue), NesB (yellow), NesC (green), and NesD (red) along with a peptide without NES (black).

(C) Bar chart represents the pre-treatment localization (blue) and post-treatment localization (red) as measured by taking the ratio of cytosol-to-nuclear fluorescent signal for peptides fused with NesA, NesB, NesC, and NesD compared to a peptide without NES.

(D) Table contains the amino acid sequences of the NES that was fused to the peptide along with the derived gene names.

All data points in this figure represent an average signal intensity calculated from 30 cells over 3 independent experiments. Error bar represents standard error of mean. * represents $p<0.001$. Scale bar represents 10 μm.

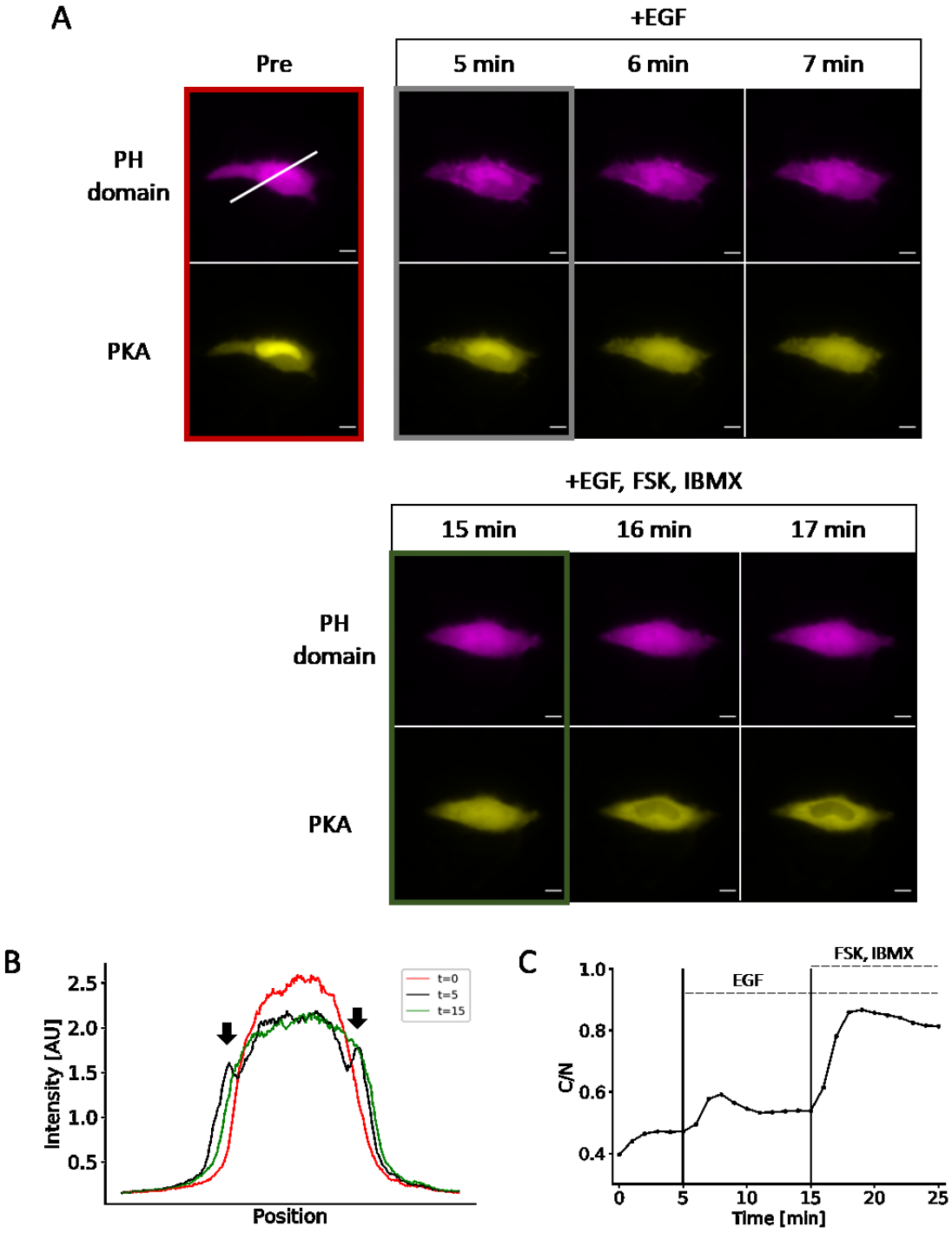
A
+EGF
Pre
5 min
6 min
7 min
PH domain
PKA
+EGF, FSK, IBMX
15 min
16 min
17 min
PH domain
PKA
B
Intensity [AU]
2.5
2.0
1.5
1.0
0.5
Position
t=0
t=5
t=15
C
FSK, IBMX
EGF
C/N
1.0
0.8
0.6
0.4
0
5
10
15
20
25
Time [min]

Figure 3-4: Duplex monitoring of PIP_3 and PKA in a single cell.

(A) Representative images show PIP_3 accumulation (as indicated by translocation of PH domain) and PKA activity in a single cell after EGF treatment followed by PKA activation.

(B) Line-scan of the image in Figure 4A (white line) shows the transient appearance of enriched fluorescent signal at the plasma membrane (arrows).

(C) Response profile shows the normalized signal change that results from EGF stimulation followed by a saturation of the reporter response with forskolin and IBMX cocktail.

Data points represent measurement from a single cell. Scale bar represents 10 μm.

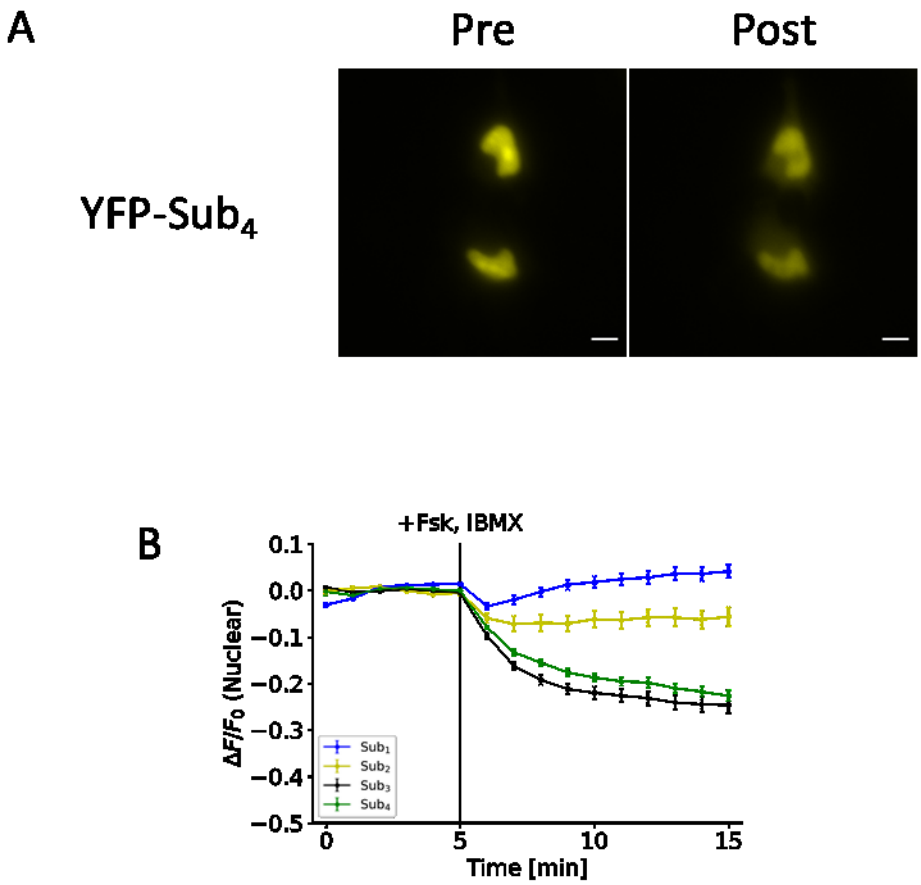

Figure 3-5: Response of tetravalent substrate to PKA activation.

(A) Representative images show the localization of YFP-Sub$_4$ pre-treatment (Pre) and 10 minutes post-treatment (Post).

(B) Response profile shows the normalized change in nuclear fluorescent signal after PKA activation with the peptides containing the different number of substrates.

All data points in this figure represent an average signal intensity calculated from 30 cells over 3 independent experiments. Error bar represents standard error of mean. Scale bar represents 10 µm.

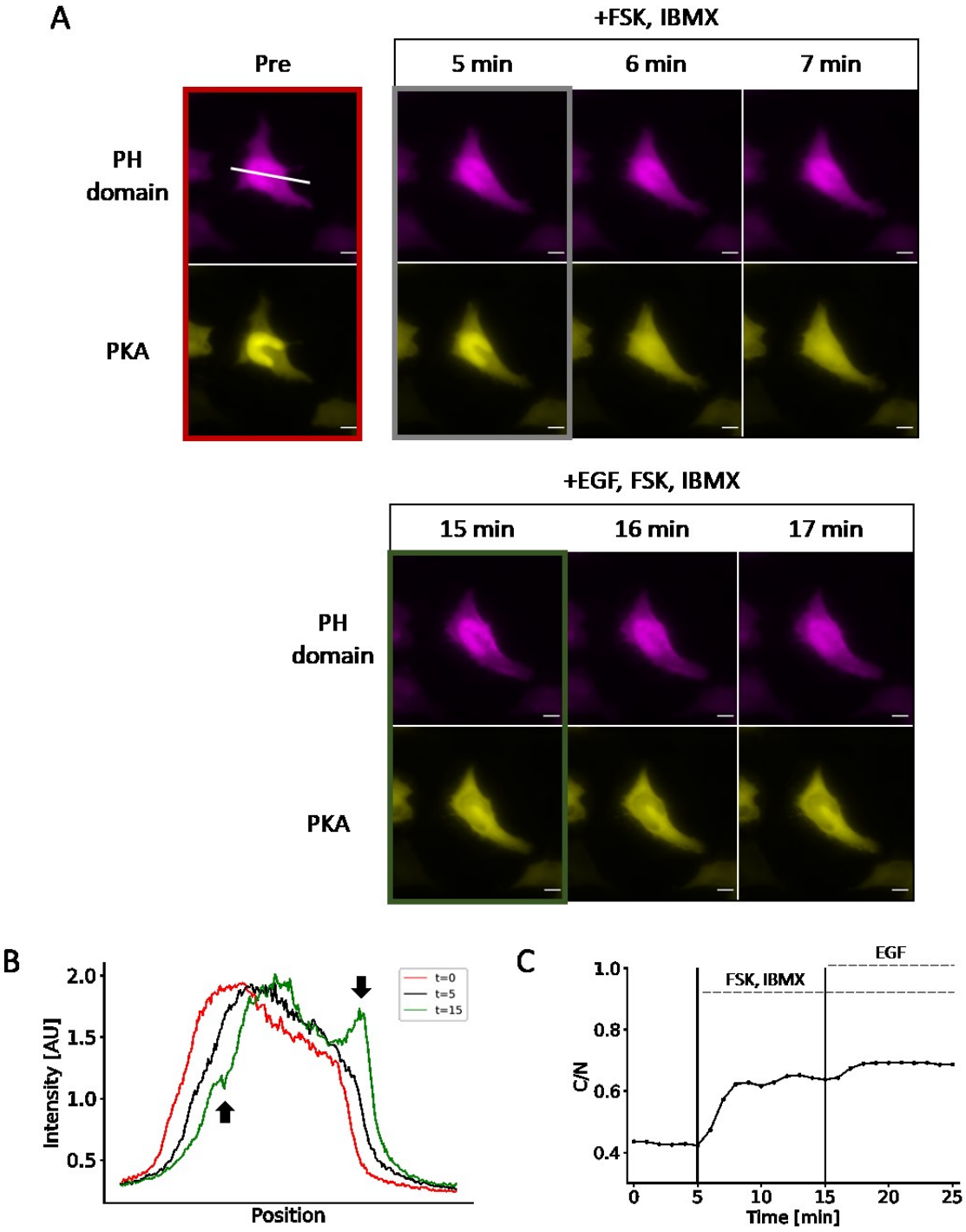
A
+FSK, IBMX
Pre
5 min
6 min
7 min
PH domain
PKA
+EGF, FSK, IBMX
15 min
16 min
17 min
PH domain
PKA
B
Intensity [AU]
2.0
1.5
1.0
0.5
Position
t=0
t=5
t=15
C
C/N
1.0
0.8
0.6
0.4
FSK, IBMX
EGF
0
5
10
15
20
25
Time [min]

<u>Figure 3-6:</u> Duplex monitoring of PIP_3 and PKA in a single cell with PKA activation followed by EGF treatment.

(A) Representative images show PKA activity and PIP_3 accumulation (as indicated by translocation of PH domain) in a single cell after PKA activation followed by EGF treatment.

(B) Line-scan of the image in Figure 4A (white line) shows the transient appearance of enriched fluorescent signal at the plasma membrane with EGF treatment but not with PKA activation (arrows).

(C) Response profile shows the normalized signal change that results from PKA activation followed by EGF stimulation.

Data points represent measurement from a single cell. Scale bar represents 10 μm.

4. Conclusion

Localization sequences are important properties of proteins that directs proteins to the correct part of a cell. These sequences contain motifs which mediate molecular interactions with other molecules within a cell. Relevant to this dissertation are the localization sequences responsible for targeting a -CAAX modified protein to the plasma membrane and the sequence responsible for nuclear localization. Both sequences utilize basic residues for their signaling properties, where introduction of phosphate groups into these regions leads to a diminishing of the signaling efficacy. By utilizing the observations of substrate recognition mechanism of basophilic kinases, it is possible to construct amino acid sequences that will respond by changing localization with phosphorylation.

Developing a farnesyl-electrostatic switch from PKA recognition motif allowed us to explore the parameters of that was not possible with the amino acid sequence natively found in the C-terminus of K-Ras4b. Protein Kinase C substrate recognition requires multiple basic residues in this region, and thus, any mutations to decrease the positive charge content changes its phosphorylability. This short peptide allowed us to explore various parameters of the prevailing model of farnesyl-electrostatic switch mechanism. By demonstrating that changing positive charges affects the switching mechanism, our data confirms the prevailing model plasma-membrane-targeting of K-Ras4b is largely due to the positive charge content in the C-terminus.

The principles here was applied similarly to a phosphorylation switch that shuttled between the cytosol and the nucleus. Nuclear localization sequences, similarly to the plasma-membrane-targeting sequence of -CAAX proteins, utilize basic residues to achieve targeting. This was used to design a kinase reporter which shuttled between the cytosol and the nucleus where phosphorylation directly regulated the nuclear localization sequence.

The work here collectively demonstrates that simple principles govern the basic property of these forms of localization in cells. Phosphorylation is a dynamic, reversible, post-translational modifications. Its ability to regulate protein property is well-characterized and understood. Here, this dissertation used the principles observed in biology to reconstruct this mechanism *de novo* using Protein Kinase A as a model kinase.

5. References

1. Crick, F. Central Dogma of Molecular Biology. *Nature* **227**, 561–563 (1970).
2. Deribe, Y. L., Pawson, T. & Dikic, I. Post-translational modifications in signal integration. *Nat. Struct. Mol. Biol.* **17**, 666–672 (2010).
3. Jensen, O. N. Interpreting the protein language using proteomics. *Nat. Rev. Mol. Cell Biol.* **7**, 391–403 (2006).
4. Chen, B., Sun, Y., Niu, J., Jarugumilli, G. K. & Wu, X. Protein Lipidation in Cell Signaling and Diseases: Function, Regulation, and Therapeutic Opportunities. *Cell Chem. Biol.* **25**, 817–831 (2018).
5. Caron, C., Boyault, C. & Khochbin, S. Regulatory cross-talk between lysine acetylation and ubiquitination: role in the control of protein stability. *BioEssays* **27**, 408–415 (2005).
6. Chen, Z. J. & Sun, L. J. Nonproteolytic Functions of Ubiquitin in Cell Signaling. *Mol. Cell* **33**, 275–286 (2009).
7. Manning, G. The Protein Kinase Complement of the Human Genome. *Science* **298**, 1912–1934 (2002).
8. Sacco, F., Perfetto, L., Castagnoli, L. & Cesareni, G. The human phosphatase interactome: An intricate family portrait. *FEBS Lett.* **586**, 2732–2739 (2012).
9. Ubersax, J. A. & Ferrell Jr, J. E. Mechanisms of specificity in protein phosphorylation. *Nat. Rev. Mol. Cell Biol.* **8**, 530–541 (2007).
10. Obata, T. *et al.* Peptide and Protein Library Screening Defines Optimal Substrate Motifs for AKT/PKB. *J. Biol. Chem.* **275**, 36108–36115 (2000).

11. Nishikawa, K., Toker, A., Johannes, F.-J., Songyang, Z. & Cantley, L. C. Determination of the Specific Substrate Sequence Motifs of Protein Kinase C Isozymes. *J. Biol. Chem.* **272**, 952–960 (1997).

12. Hutti, J. E. *et al.* A rapid method for determining protein kinase phosphorylation specificity. *Nat. Methods* **1**, 27–29 (2004).

13. Kemp, B. E., Graves, D. J., Benjamini, E. & Krebs, E. G. Role of multiple basic residues in determining the substrate specificity of cyclic AMP-dependent protein kinase. *J. Biol. Chem.* **252**, 4888–4894 (1977).

14. Good, M. C., Zalatan, J. G. & Lim, W. A. Scaffold Proteins: Hubs for Controlling the Flow of Cellular Information. *Science* **332**, 680–686 (2011).

15. Boeynaems, S. *et al.* Protein Phase Separation: A New Phase in Cell Biology. *Trends Cell Biol.* **28**, 420–435 (2018).

16. Kallunki, T., Deng, T., Hibi, M. & Karin, M. c-Jun Can Recruit JNK to Phosphorylate Dimerization Partners via Specific Docking Interactions. *Cell* **87**, 929–939 (1996).

17. Tanoue, T., Adachi, M., Moriguchi, T. & Nishida, E. A conserved docking motif in MAP kinases common to substrates, activators and regulators. *Nat. Cell Biol.* **2**, 110–116 (2000).

18. Reményi, A., Good, M. C. & Lim, W. A. Docking interactions in protein kinase and phosphatase networks. *Curr. Opin. Struct. Biol.* **16**, 676–685 (2006).

19. Ahearn, I. M., Haigis, K., Bar-Sagi, D. & Philips, M. R. Regulating the regulator: post-translational modification of RAS. *Nat. Rev. Mol. Cell Biol.* **13**, 39–51 (2012).

20. Bivona, T. G. *et al.* PKC Regulates a Farnesyl-Electrostatic Switch on K-Ras that Promotes its Association with Bcl-Xl on Mitochondria and Induces Apoptosis. *Mol. Cell* **21**, 481–493 (2006).

21. Kosugi, S. *et al.* Six Classes of Nuclear Localization Signals Specific to Different Binding Grooves of Importin α. *J. Biol. Chem.* **284**, 478–485 (2009).

22. Lange, A. *et al.* Classical Nuclear Localization Signals: Definition, Function, and Interaction with Importin α. *J. Biol. Chem.* **282**, 5101–5105 (2007).

23. Nardozzi, J. D., Lott, K. & Cingolani, G. Phosphorylation meets nuclear import: a review. *Cell Commun. Signal.* **8**, 32 (2010).

24. Harreman, M. T. *et al.* Regulation of Nuclear Import by Phosphorylation Adjacent to Nuclear Localization Signals. *J. Biol. Chem.* **279**, 20613–20621 (2004).

25. Ahearn, I. M., Haigis, K., Bar-Sagi, D. & Philips, M. R. Regulating the regulator: post-translational modification of RAS. *Nat. Rev. Mol. Cell Biol.* **13**, 39–51 (2012).

26. Wright, L. P. & Philips, M. R. CAAX modification and membrane targeting of Ras. *J. Lipid Res.* **47**, 883–891 (2006).

27. Choy, E. *et al.* Endomembrane Trafficking of Ras. *Cell* **98**, 69–80 (1999).

28. Gomez, G. A. & Daniotti, J. L. Electrical properties of plasma membrane modulate subcellular distribution of K-Ras: Membrane targeting of K-Ras. *FEBS J.* **274**, 2210–2228 (2007).

29. Hancock, J. F., Paterson, H. & Marshall, C. J. A polybasic domain or palmitoylation is required in addition to the CAAX motif to localize p21ras to the plasma membrane. *Cell* **63**, 133–139 (1990).

30. Heo, W. D. *et al.* PI(3,4,5)P3 and PI(4,5)P2 Lipids Target Proteins with Polybasic Clusters to the Plasma Membrane. *Science* **314**, 1458–1461 (2006).

31. Leventis, R. & Silvius, J. R. Lipid-Binding Characteristics of the Polybasic Carboxy-Terminal Sequence of K- *ras* 4B †. *Biochemistry* **37**, 7640–7648 (1998).

32. Roy, M.-O., Leventis, R. & Silvius, J. R. Mutational and Biochemical Analysis of Plasma Membrane Targeting Mediated by the Farnesylated, Polybasic Carboxy Terminus of K-ras4B †. *Biochemistry* **39**, 8298–8307 (2000).

33. Yeung, T. *et al.* Membrane Phosphatidylserine Regulates Surface Charge and Protein Localization. *Science* **319**, 210–213 (2008).

34. Bivona, T. G. *et al.* PKC Regulates a Farnesyl-Electrostatic Switch on K-Ras that Promotes its Association with Bcl-Xl on Mitochondria and Induces Apoptosis. *Mol. Cell* **21**, 481–493 (2006).

35. Jang, H. *et al.* Mechanisms of Membrane Binding of Small GTPase K-Ras4B Farnesylated Hypervariable Region. *J. Biol. Chem.* **290**, 9465–9477 (2015).

36. Schmick, M. *et al.* KRas Localizes to the Plasma Membrane by Spatial Cycles of Solubilization, Trapping and Vesicular Transport. *Cell* **157**, 459–471 (2014).

37. Kemp, B. E., Graves, D. J., Benjamini, E. & Krebs, E. G. Role of multiple basic residues in determining the substrate specificity of cyclic AMP-dependent protein kinase. *J. Biol. Chem.* **252**, 4888–4894 (1977).

38. Hutti, J. E. *et al.* A rapid method for determining protein kinase phosphorylation specificity. *Nat. Methods* **1**, 27–29 (2004).

39. Hicks, K. A., Hartman, H. L. & Fierke, C. A. Upstream Polybasic Region in Peptides Enhances Dual Specificity for Prenylation by Both Farnesyltransferase and Geranylgeranyltransferase Type I. *Biochemistry* **44**, 15325–15333 (2005).

40. Zhang, F. L. *et al.* Characterization of Ha-Ras, N-Ras, Ki-Ras4A, and Ki-Ras4B as in Vitro Substrates for Farnesyl Protein Transferase and Geranylgeranyl Protein Transferase Type I. *J. Biol. Chem.* **272**, 10232–10239 (1997).

41. Kemp, B. E. & Pearson, R. B. Protein kinase recognition sequence motifs. *Trends Biochem. Sci.* **15**, 342–346 (1990).

42. Fivaz, M. Reversible intracellular translocation of KRas but not HRas in hippocampal neurons regulated by Ca2+/calmodulin. *J. Cell Biol.* **170**, 429–441 (2005).

43. Villalonga, P. *et al.* Calmodulin Binds to K-Ras, but Not to H- or N-Ras, and Modulates Its Downstream Signaling. *Mol. Cell. Biol.* **21**, 7345–7354 (2001).

44. Abraham, S. J., Nolet, R. P., Calvert, R. J., Anderson, L. M. & Gaponenko, V. The Hypervariable Region of K-Ras4B Is Responsible for Its Specific Interactions with Calmodulin. *Biochemistry* **48**, 7575–7583 (2009).

45. Sperlich, B., Kapoor, S., Waldmann, H., Winter, R. & Weise, K. Regulation of K-Ras4B Membrane Binding by Calmodulin. *Biophys. J.* **111**, 113–122 (2016).

46. Komatsu, N. *et al.* Development of an optimized backbone of FRET biosensors for kinases and GTPases. *Mol. Biol. Cell* **22**, 4647–4656 (2011).

47. Zhou, Y. *et al.* Lipid-Sorting Specificity Encoded in K-Ras Membrane Anchor Regulates Signal Output. *Cell* **168**, 239-251.e16 (2017).

48. Schmick, M. *et al.* KRas Localizes to the Plasma Membrane by Spatial Cycles of Solubilization, Trapping and Vesicular Transport. *Cell* **157**, 459–471 (2014).

49. Chandra, A. *et al.* The GDI-like solubilizing factor PDEδ sustains the spatial organization and signalling of Ras family proteins. *Nat. Cell Biol.* **14**, 148–158 (2012).

50. Zimmermann, G. *et al.* Small molecule inhibition of the KRAS–PDEδ interaction impairs oncogenic KRAS signalling. *Nature* **497**, 638–642 (2013).

51. Sidhu, R. S., Clough, R. R. & Bhullar, R. P. Ca2+/calmodulin binds and dissociates K-RasB from membrane. *Biochem. Biophys. Res. Commun.* **304**, 655–660 (2003).

52. Perera, R. K. & Nikolaev, V. O. Compartmentation of cAMP signalling in cardiomyocytes in health and disease. *Acta Physiol.* **207**, 650–662 (2013).

53. Park, H. & Poo, M. Neurotrophin regulation of neural circuit development and function. *Nat. Rev. Neurosci.* **14**, 7–23 (2013).

54. Sethi, J. K. & Vidal-Puig, A. J. *Thematic review series: Adipocyte Biology.* Adipose tissue function and plasticity orchestrate nutritional adaptation. *J. Lipid Res.* **48**, 1253–1262 (2007).

55. Wong, W. & Scott, J. D. AKAP signalling complexes: focal points in space and time. *Nat. Rev. Mol. Cell Biol.* **5**, 959–970 (2004).

56. Zaccolo, M. Discrete Microdomains with High Concentration of cAMP in Stimulated Rat Neonatal Cardiac Myocytes. *Science* **295**, 1711–1715 (2002).

57. Zhang, J., Ma, Y., Taylor, S. S. & Tsien, R. Y. Genetically encoded reporters of protein kinase A activity reveal impact of substrate tethering. *Proc. Natl. Acad. Sci.* **98**, 14997–15002 (2001).

58. Zhang, J., Hupfeld, C. J., Taylor, S. S., Olefsky, J. M. & Tsien, R. Y. Insulin disrupts β-adrenergic signalling to protein kinase A in adipocytes. *Nature* **437**, 569–573 (2005).

59. Allen, M. D. & Zhang, J. Subcellular dynamics of protein kinase A activity visualized by FRET-based reporters. *Biochem. Biophys. Res. Commun.* **348**, 716–721 (2006).

60. Depry, C., Allen, M. D. & Zhang, J. Visualization of PKA activity in plasma membrane microdomains. *Mol BioSyst* **7**, 52–58 (2011).

61. Tillo, S. E. *et al.* Liberated PKA Catalytic Subunits Associate with the Membrane via Myristoylation to Preferentially Phosphorylate Membrane Substrates. *Cell Rep.* **19**, 617–629 (2017).

62. Aye-Han, N.-N., Allen, M. D., Ni, Q. & Zhang, J. Parallel tracking of cAMP and PKA signaling dynamics in living cells with FRET-based fluorescent biosensors. *Mol. Biosyst.* **8**, 1435 (2012).

63. Ross, B. L. *et al.* Single-color, ratiometric biosensors for detecting signaling activities in live cells. *eLife* **7**, (2018).

64. Regot, S., Hughey, J. J., Bajar, B. T., Carrasco, S. & Covert, M. W. High-Sensitivity Measurements of Multiple Kinase Activities in Live Single Cells. *Cell* **157**, 1724–1734 (2014).

65. Henderson, B. R. & Eleftheriou, A. A Comparison of the Activity, Sequence Specificity, and CRM1-Dependence of Different Nuclear Export Signals. *Exp. Cell Res.* **256**, 213–224 (2000).

66. Blom, N., Sicheritz-Pontén, T., Gupta, R., Gammeltoft, S. & Brunak, S. Prediction of post-translational glycosylation and phosphorylation of proteins from the amino acid sequence. *PROTEOMICS* **4**, 1633–1649 (2004).

6. Curriculum Vitae

Allen Kyung Kim

Educational History:

PhD (expected)	2019	Biomedical Engineering Mentor: Takanari Inoue	Johns Hopkins School of Medicine
MEng	2011	Biomedical Engineering	Cornell University
BS	2010	Engineering Physics	Cornell University

Other Professional Experiences:

2011-2013	Lab of Peipei Ping, University of California, Los Angeles

Academic Honors:

2010-2011	MEC Fellowship, College of Engineering
2010	Department Honor, Applied and Engineering Physics, Cornell University
2006-2010	Dean's List, College of Engineering, Cornell University (7 of 8)

Publications:

Kim AK, Inoue T. Rational design of a Protein Kinase A nuclear-cytosol translocation reporter. bioRxiv (2019). doi:10.1101/709766 (Preprint)

Kim AK, Inoue T. Rational design of a synthetic farnesyl-electrostatic switch based on the hypervariable region of K-Ras4b. bioRxiv (2019). doi:10.1101/635839 (Preprint)

Miyamoto T, Rho E, Kim A, Inoue T. Cellular Application of Genetically Encoded Sensors and Impeders of AMPK. Methods Mol Biol. 2018; 1732:255-272. doi: 10.1007/978-1-4939-7598-3_17. PubMed PMID: 29480481.

Kim AK, DeRose R, Ueno T, Lin B, Komatsu T, Nakamura H, Inoue T. Toward total synthesis of cell function: Reconstituting cell dynamics with synthetic biology. Science signaling. 2016; 9(414):re1. PubMed [journal] PMID: 26861045

Lam MP, Wang D, Lau E, Liem DA, Kim AK, Ng DC, Liang X, Bleakley BJ, Liu C, Tabaraki JD, Cadeiras M, Wang Y, Deng MC, Ping P. Protein kinetic signatures of the remodeling heart following isoproterenol stimulation. The Journal of clinical investigation. 2014; 124(4):1734-44. PubMed [journal] PMID: 24614109, PMCID: PMC3973111

Wang D, Fang C, Zong NC, Liem DA, Cadeiras M, Scruggs SB, Yu H, Kim AK, Yang P, Deng M, Lu H, Ping P. Regulation of acetylation restores proteolytic function of diseased myocardium in mouse and human. Molecular & cellular proteomics: MCP. 2013; 12(12):3793-802. PubMed [journal] PMID: 24037710, PMCID: PMC3861724

Zong NC, Li H, Li H, Lam MP, Jimenez RC, Kim CS, Deng N, Kim AK, Choi JH, Zelaya I, Liem D, Meyer D, Odeberg J, Fang C, Lu HJ, Xu T, Weiss J, Duan H, Uhlen M, Yates JR 3rd, Apweiler R, Ge J, Hermjakob H, Ping P. Integration of cardiac proteome biology and medicine by a specialized knowledgebase. Circulation research. 2013; 113(9):1043-53. NIHMSID: NIHMS526610 PubMed [journal] PMID: 23965338, PMCID: PMC4076475

Li H, Zong NC, Liang X, Kim AK, Choi JH, Deng N, Zelaya I, Lam M, Duan H, Ping P. A novel spectral library workflow to enhance protein identifications. Journal of proteomics. 2013; 81:173-84. NIHMSID: NIHMS452749 PubMed [journal] PMID: 23391412, PMCID: PMC3737079

Kim TY, Wang D, Kim AK, Lau E, Lin AJ, Liem DA, Zhang J, Zong NC, Lam MP, Ping P. Metabolic labeling reveals proteome dynamics of mouse mitochondria. Molecular & cellular proteomics: MCP. 2012; 11(12):1586-94. PubMed [journal] PMID: 22915825, PMCID: PMC3518123

Bazarov IV, Kim A, Lakshmanan MN, Maxson JM. Comparison of DC and SRF photoemission guns for high brightness high average current beam production. Physical review accelerators and beams. 2011; 14:072001.

Patents:

Ping P, Kim T-Y, Wang D, Kim A, Lau E, Liem DA, Lam PY, D M. "Method for Determination of Biomolecule Turnover Rates" US20180372753A1 (Pending).